CrossMark

ORIGINAL RESEARCH PAPER

Probabilistic seismic hazard assessment for South-Eastern France

Christophe Martin[1] · Gabriele Ameri[1] ⬤ · David Baumont[1] ·
David Carbon[1] · Gloria Senfaute[2] · Jean-Michel Thiry[3,6] ·
Ezio Faccioli[4] · Jean Savy[5]

Abstract The accurate evaluation and appropriate treatment of uncertainties is of primary importance in modern probabilistic seismic hazard assessment (PSHA). One of the objectives of the SIGMA project was to establish a framework to improve knowledge and data on two target regions characterized by low-to-moderate seismic activity. In this paper, for South-Eastern France, we present the final PSHA performed within the SIGMA project. A new earthquake catalogue for France covering instrumental and historical periods was used for the calculation of the magnitude-frequency distributions. The hazard model incorporates area sources, smoothed seismicity and a 3D faults model. A set of recently developed ground motion prediction equations (GMPEs) from global and regional data, evaluated as adequately representing the ground motion characteristics in the region, was used to calculate the hazard. The magnitude-frequency distributions, maximum magnitude, faults slip rate and style-of-faulting are considered as additional source of epistemic uncertainties. The hazard results for generic rock condition (Vs30 = 800 m/s) are displayed for 20 sites in terms of uniform hazard spectra at two return periods (475 years and 10,000 years). The contributions of the epistemic uncertainties in the ground motion characterizations and in the seismic source characterization to the total hazard uncertainties are analyzed. Finally, we compare the results with existing models developed at national

✉ Gabriele Ameri
  g.ameri@fugro.com

[1] Geoter SAS - Fugro, 13390 Auriol, France

[2] EDF-CEIDRE-TEGG, Aix-en-Provance, France

[3] AREVA, 69456 Lyon, France

[4] Studio Geotecnico Italiano, 20141 Milan, Italy

[5] Savy Risk Consulting, Oakland, CA 94610, USA

[6] Present Address: Apave Sudeurope SAS, Paris, France

🙆 Springer

scale in the framework of the first generation of models supporting the Eurocode 8 enforcement, (MEDD 2002 and AFPS06) and at the European scale (within the SHARE project), highlighting significant discrepancies at short return periods.

Keywords PSHA · France · Uncertanties · Sigma

1 Introduction

One of the objectives of the SIGMA project (Pecker et al. 2017) was to create a European scientific framework involving earth scientists, engineers and consultants to better understand the role of the uncertainties in Probabilistic Seismic Hazard Assessment (PSHA), to improve the robustness of the PSHA estimates and to identify the future challenges in carrying out PSHA in low-to-moderately active seismic areas.

The SIGMA project was organized around five complementary work packages two of which focusing on the improvement of the earthquake catalogue and the knowledge of seismic sources (WP1) and on the development of ground motion models (WP2). Two regions were selected for the development of models and the calculation of hazard with due consideration of the contributions of the work packages: the South-Eastern France and the Po Plain in Northern Italy. Because the amount of regional and site-specific data was notably different in the two regions—the Po plain benefiting from more complete fault database, dense seismic network, and empirical ground motion database collected during recent events—the two models were developed with different objectives. For the Po plain, the construction of the logic tree was much more data-driven and advanced analyses were introduced: rupture simulations, seismic sources modelled as faults rather than area sources, host-to-target adjustments and single-station sigma approach (Faccioli et al. 2015; Vanini et al. 2017). In the case of South-Eastern France, although extensive sensitivity analyses studies were conducted (Ameri et al. 2014), the logic-tree development was much more governed by the new inputs generated by the WP1 and WP2. This paper presents the model developed for South-Eastern France.

While not comparable to the formal SSHAC methodology (Budnitz et al. 1997) nowadays applied to carry out site-specific PSHA for critical structures, the approach used in this study seeks to capture the diversity of the scientific opinions. Indeed the SIGMA project was organized in such way that scientists, consultants, resource and proponent experts had the opportunity to exchange their views and works during bi-annual scientific committee meetings, and activities and reports were continuously reviewed by members of this committee. In order to identify the parameters and associated uncertainties controlling the seismic hazard estimates and their variability and to be able to measure the benefits of the SIGMA research and development actions, at an early stage of the project it was decided to develop a PSHA model representing the state of practice. This model was used to conduct extensive sensitivity analyses considering various data, parameters and hypothesis. It evolved continuously to integrate the contributions of the work packages as well as the positions and opinions explained by the proponent experts and by the reviewers.

The present paper mainly focuses on the results obtained with the final logic tree although the different evolutions of the models remain available in the SIGMA project deliverables. To estimate the hazard variability at regional scale, the hazard results are displayed for 20 sites in terms of uniform hazard spectra (UHS) at two return periods. The contributions of the epistemic uncertainties in the GMC and in the SSC to the total hazard uncertainties are analyzed. In order to evaluate the impact of the new hazard model, we

finally compare the new results with existing models developed at national scale in the framework of the first generation of models supporting the Eurocode 8 enforcement, (MEDD 2002 and AFPS06) and at the European scale (SHARE 2013, Woessner et al. 2015), highlighting significant discrepancies at short return periods.

2 Treatment of the SIGMA earthquake catalogue

The earthquake catalogue has been developed through an iterative process, which led to the development of several versions to account for the comments and issues raised during the review process. The version used in this study was delivered by WP1 after the final scientific committee meeting of the SIGMA project. The difference between the version used here and the final version (Manchuel et al. 2017) is essentially related to the strategy to define the fixed depth for historical events with limited amount of macroseismic data (K. Manchuel, written communication) and should not affect significantly the analyses conducted in this study. The earthquake catalogue covers the metropolitan France in the time interval 463–2009 with a reference magnitude scale in Mw. It results from the merge of the SI-Hex instrumental seismic catalogue (Cara et al. 2015) and of the parametric historical earthquakes catalogue developed in the framework of the SIGMA project (Manchuel et al. 2017). This latter component is the product of an integrated study on historical seismicity including the calibration of intensity attenuation models for the French territory (Baumont et al. 2017), and the development of the logic tree to specifically account for the epistemic uncertainties (Traversa et al. 2017) and its application to the SISFRANCE macroseismic data (Manchuel et al. 2017). This section briefly describes the treatment of the earthquake catalogue in order to remove dependent events (i.e., foreshocks and aftershocks) and to determine completeness periods.

The catalogue declustering is performed using standard approaches based on the temporal and spatial windows proposed by Gardner and Knopoff (1974). The procedure relates the maximum possible distance and time of an aftershock to the main shock magnitude. Temporal and spatial windows by Gardner and Knopoff (1974) are defined by the following equations (Van Stiphout et al. 2012):

$$d = 10^{0.1238*M+0.983}$$
$$t = 10^{0.032*M+2.7389} \quad \text{for } M \geq 6.5$$
$$t = 10^{0.5409*M-0.547} \quad \text{else}$$

where d is the distance window in km, t is time window in days and M is the moment magnitude on the main event. The initial catalogue is composed by 48,704 events. The declustered catalogue is composed by 35,694 main events meaning that about 25% of the events in the original catalogue are aftershocks and foreshocks. Figure 1 shows the declustered catalogue in the study region and the 20 target sites selected within this project for the PSHA calculations.

The completeness periods of the catalogue are important input parameters that identify which part of the catalogue can be considered complete (reporting all the earthquakes that actually occurred for a given magnitude class). This is fundamental information in order to apply time-independent recurrence model that imply a stationary seismicity with time. The assessment of completeness is usually performed according to statistical analyses of the catalogues (e.g. Stepp 1972; Musson 1999; Albarello et al. 2001), based on the assumption that the seismogenic process is stationary. The determination of completeness periods is
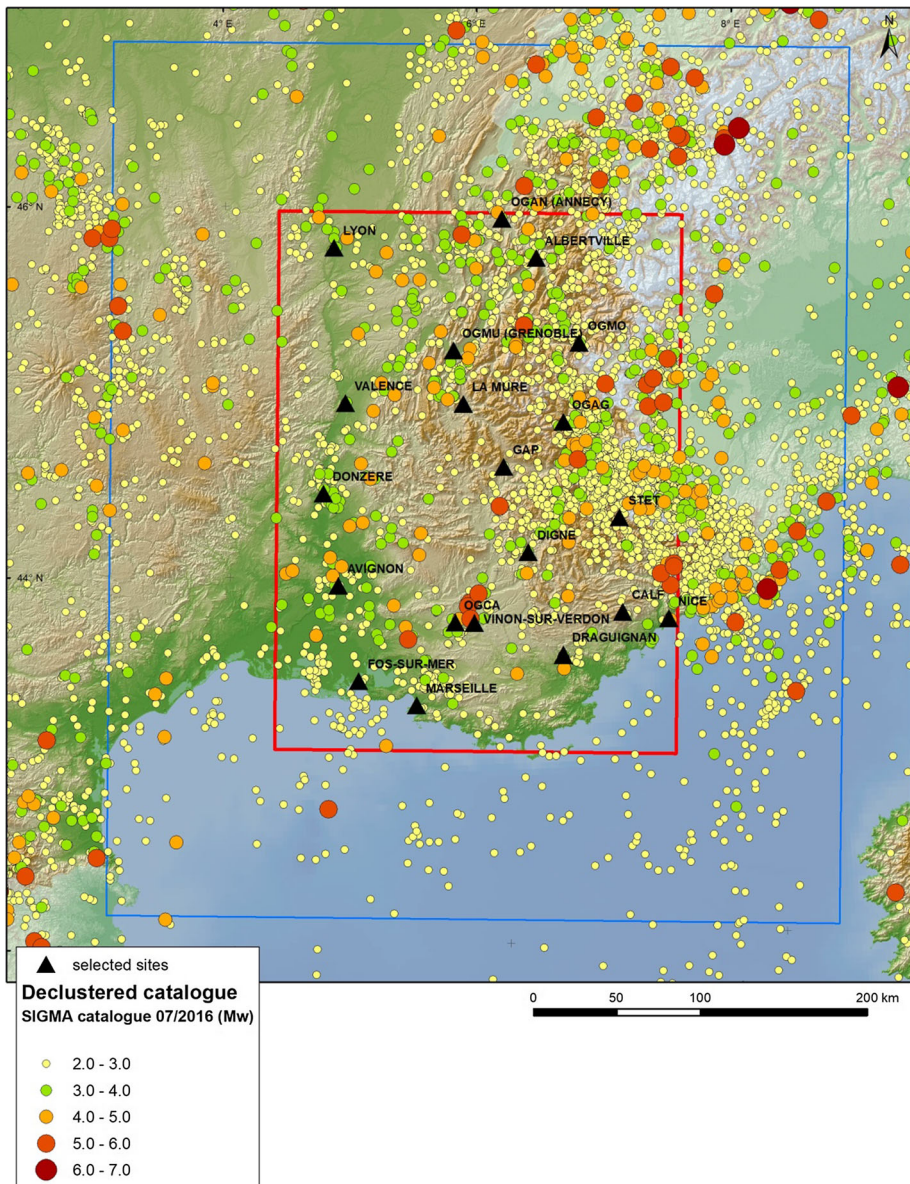
Fig. 1 SIGMA declustered earthquake catalogue in the study area. Black triangles represent the 20 sites selected for PSHA

based on the statistical analysis of number of earthquakes per magnitude bin over time. Completeness periods are estimated from the analysis of the cumulative number of events over time (e.g., Burkhard and Grünthal 2009; Grünthal et al. 2010) combined with the analysis of the standard deviation of the estimate of the mean rate of earthquakes over time (Stepp 1972). This allows us to estimate the year from which the catalogue is considered complete for a given magnitude range. Based on the regional context of the study, the

determination of completeness is performed separating the catalogue in two completeness superzones according to the population density. The zones of the Alps and offshore are characterized by a lower population density and thus it is expected that a shorter completeness period is obtained for the historical earthquakes, especially for small magnitude events.

The years of completeness and relative uncertainties as a function of magnitude for low-population density and high-population density superzones are reported in Table 1. The values estimated in this study are in good agreement with those estimated in the SHARE project, especially for large magnitudes. The uncertainty values are assigned associating smaller uncertainties to small magnitude ranges for which the completeness periods are easier to determine, due to the larger data sample. Based on visual analysis of the cumulative distributions and on expert judgement, three uncertainty values are assigned:

- ± 5 years for Mw < 3.5;
- ± 25 years for $3.5 \leq Mw \leq 5.0$;
- ± 50 years for Mw > 5.0

The uncertainties in the determination of the completeness periods are considered in the calculation of the magnitude-frequency distributions (MFDs), as detailed in the following of the paper.

3 Seismic source characterization (SSC)

The SSC model has been developed based on the evaluation and integration of recent published studies on the subject trying to capture the alternative interpretations of the French and international scientific communities.

According to the state-of-the-art of PSHA, three types of seismic source models are used: area source models, 3D fault models and smoothed seismicity models. Concerning the fault model, due to the relative poor knowledge of fault sources in the target region, it was only developed in Provence (Middle Durance fault and compressive structures of Provence region) thus affecting the hazard in a relatively small region.

Table 1 Adopted completeness years (± uncertainty) as a function of magnitude and population density

Mw ($\geq$)	Year of completeness low population	Mw ($\geq$)	Year of completeness high population
2.0	1965 $\pm$ 5 years	2.0	1965 $\pm$ 5 years
2.5	1963 $\pm$ 5 years	2.5	1963 $\pm$ 5 years
3.0	1950 $\pm$ 5 years	3.0	1900 $\pm$ 5 years
3.5	1896 $\pm$ 25 years	3.5	1857 $\pm$ 25 years
4.0	1850 $\pm$ 25 years	4.0	1850 $\pm$ 25 years
4.5	1850 $\pm$ 25 years	4.5	1800 $\pm$ 25 years
5.0	1770 $\pm$ 25 years	5.0	1700 $\pm$ 25 years
5.5	1500 $\pm$ 50 years	5.5	1500 $\pm$ 50 years
6.1	1300 $\pm$ 50 years	5.7	1450 $\pm$ 50 years
		6.1	1300 $\pm$ 50 years

3.1 Area source models

Area sources represent regions exhibiting the same seismotectonic regime and seismicity occurrence features. They are modeled assuming that the seismicity is homogenously distributed over their extent and the occurrence parameters are calculated by processing the subset of events that occurred within the polygon describing the seismic source. This procedure necessarily suffer of the trade-off between the need for small areas, to guarantee that the underlying seismogenic process is properly considered, and the need for large enough area sources, to select a seismicity sample that allows a reliable calculation of the MFDs. One major criticism to area sources is that subjectivity is implicitly assumed in the definition of their geometry, especially when a unique team is responsible for the model elaboration.

To overpass this difficulty, three area source (AS) models were considered employing different criteria for the delineation of the seismic sources. These AS models represent different technical interpretations of the scientific community and have evolved during the course of the SIGMA project based on new available data and publications.

The first model (SM1) is based on Geoter studies and interpretations of the available databases in the region of interest and combines the parameters characterizing the static and dynamic states of the crust (Carbon et al. 2012). SM1 is based on the previous model developed in 2002 to produce the probabilistic seismic zonation for Eurocode 8 application (Martin et al. 2002). This model has continuously evolved in the framework of different PSHA studies in France, to integrate the results of new research and development programs. The AS model is mainly constrained by the main structural limits, the distribution of the seismicity, the kinematics of the recent and current deformations (neotectonic data, earthquake focal mechanisms), and by the geometry and characteristics of the main regional fault systems.

The second model (SM2) gives more emphasis to known or assumed fault systems and to the seismic activity as identified by the distribution of historical and instrumental earthquakes. In particular, it considers the potential relationships between the seismicity distribution and tectonic faults in three specific areas of the region of interest: (1) the alpine west front, (e.g. the Belledonne fault); (2) the western Provence (e.g., Nîme fault, Middle-Durance Fault); (3) the Tricastin cluster. The zones encompassing faults systems are identified based on published studies. For the Provence region, the studies by Clement et al. (2009), Terrier (2006), Le Pichon and Rangin (2010), Rangin et al. (2010) were used to identify the fault systems characterized by the same type of seismic deformation. This model involves seismic sources localized along the main faults of Western Provence identified as potentially active during the Plio-Quaternary period. For the alpine western front, Thouvenot et al. (2003) suggests that the recent seismicity in the Grenoble region could be associated to a bordering N30° fault of the Belledonne massif that was unidentified before, because of the important sedimentary cover, but was revealed thanks to the precise hypocenter locations of the Sismalp network (https://sismalp.osug.fr/). For the Tricastin cluster, the models developed by Clement et al. (2004) together with the analysis of instrumental seismicity done by Thouvenot et al. (2009) is used to assign the seismicity to a hypothetic fault zone. The remaining of the area source model is based on original models from other French institutions (BRGM: Bles et al. 1998, EDF and IRSN: Baize et al. 2011) that were developed to carry out deterministic assessments in application of the French Nuclear Safety rule (RFS 2001-01 (2001)). Overall, the size of the source zones in SM2 is smaller compared to SM1;

The third model (SM3) is the IRSN model as published by Baize et al. (2013) used here in the "aggregated" version as proposed by the authors. This model is much more based on the identification of a coherent structural scheme and deformation scheme under the present state of stress. It overpasses the ambiguity that affects the seismogenic potential and seismic activity in small areas, the delineation of which is sometimes based on unclear tectonic or structural limits. Seismic sources are larger than in the two previous models and it allows to work with a more complete seismic sample. Note that only the geometrical properties of the zones are taken from Baize et al. (2013) whereas the activity rates parameters are calculated in this study based on the SIGMA catalogue.

The geometry of area source models SM1, SM2 and SM3 is presented in Fig. 2. The zones names, the minimum and maximum seismogenic depths, the faulting mechanism and other information considered for each zone of SM1, SM2 and SM3 and reported in the Electronic supplement to this paper.
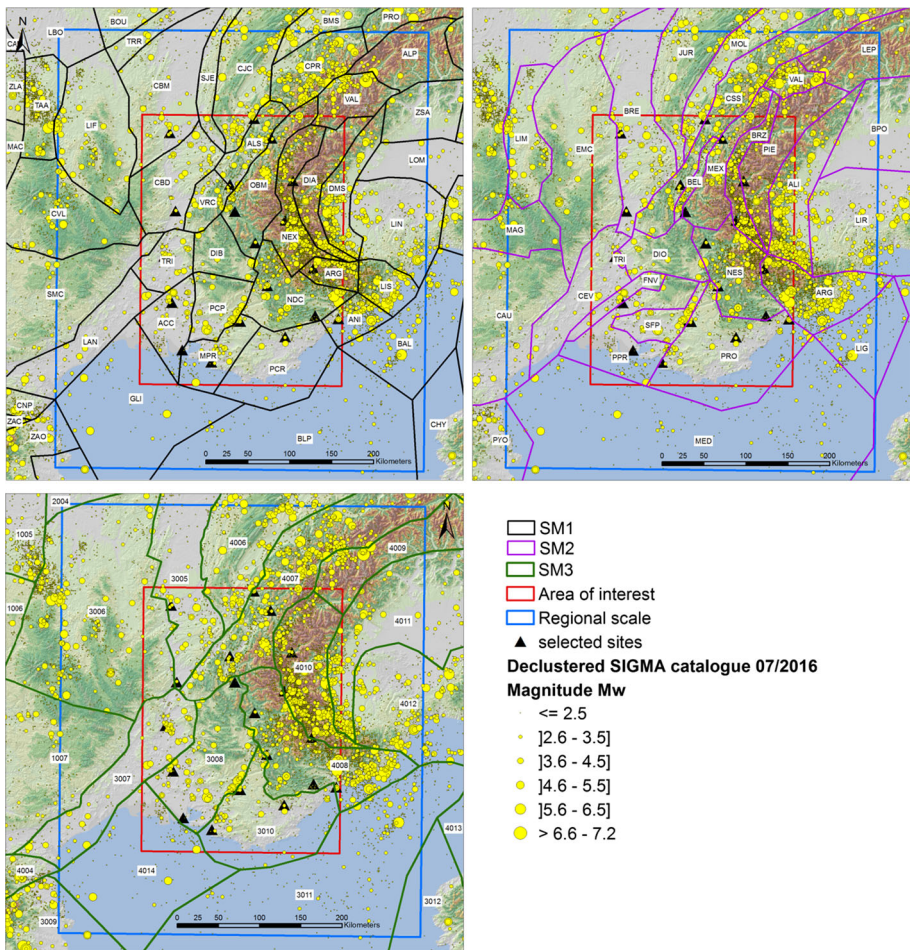

Fig. 2 Area source models (SM1, SM2 and SM3) considered for the study region. The declustered earthquake catalogue and the target sites are also shown

3.1.1 Rupture size, style of faulting and geometry of ruptures

At each grid point within an area source polygon, a set of virtual faults is generated using the depth distribution defined for each zone (as discussed in the next section). The geometry of the virtual fault is magnitude-dependent and derived from the empirical scaling relation of Wells and Coppersmith (1994). The length and width of the fault are consistent with the scaling relation until the fault rupture reaches an edge of the volume source. Then the aspect ratio will be modified to allow the fault dimensions to increase according to limits imposed by the seismogenic volume. The various types of source-to-site distances commonly used in the GMPEs are calculated for each fault geometry. The style-of-faulting, strike and dip of ruptures is described for each source zone, including both aleatory and epistemic uncertainties.

The aleatory variability for the strike and dip of the virtual faults is considered by assuming all possible fault strike angles between 0°–360° and the following variability for the dip angles according to the dominant style-of-faulting:

- For strike-slip fault mechanism: DIP MIN = 70°–MAX = 90°;
- For normal fault mechanism: DIP MIN = 50°–MAX = 70°;
- For reverse fault mechanism: DIP MIN = 30°–MAX = 50°.

For area sources characterized by mixed fault mechanism (e.g., strike-slip/reverse), a weight of 0.5 is assigned to the each mechanism (epistemic uncertainties).

The simulated hypocenters sample the volume of each area source. However, the virtual faults associated to the earthquake scenario of interest can eventually cross the boundary of the source (i.e., leaky boundary conditions). Alternatively, the fault rupture can be forced to remain fully included within the zone (i.e., strict boundary conditions). In this study, we assumed strict boundary conditions of area sources in the Alps region and leaky boundary conditions for area sources elsewhere. The main motivation is that we consider the limit of the French side of the Alps to be a major transition zone in the study region marking very different structural and seismotectonic environments. Therefore, we consider that the seismic activity of the Alps regions should remain confined within its boundaries. The type of boundary condition for each area source is reported in the electronic supplement.

3.1.2 Focal depths distribution for future earthquakes

Both epistemic and aleatory uncertainties are considered for earthquakes depth. The minimum and maximum depths within which the earthquake hypocenter is located are epistemic uncertainties. They are typically different from one area source model to another and they represent different alternative interpretation of the thickness of the seismogenic layer across the region (see the electronic supplement). On the other hand, how the earthquakes are distributed within the seismogenic layer is treated as an aleatory uncertainty. Within the seismic source zones, the depth distribution of future earthquake focal depths is defined by specifying the desired distribution that can be magnitude-dependent. During the course of the project, a statistical analysis on earthquake depths as reported in the SI-Hex instrumental catalogue was performed for different activity domains in the area of interest. Due to the relatively small number of events with Mw larger than 3.5–4.0 recorded in the last 50 years, in particular for low-seismicity areas, it was hard to establish any statistical conclusion on the depth distribution of earthquakes for magnitudes of interest for the PSHA. Nevertheless, from the analysis of the earthquake depths in the active domains (Alps) we obtain some indications on the fact that Mw larger than five

typically occur at greater depth. This is also in agreement with magnitude-dependent depth distributions employed in the PEGASOS Refinement Project (http://www.swissnuclear.ch/de/downloads.html). Thus, the following depth distribution is implemented:

- for Mw ≤ 5.5 a uniform distribution between the minimum and maximum depths for each zone;
- for larger Mw, the weights of 0.2, 0.4 and 0.4 are used for the minimum depth, mean depth and maximum depth, respectively in each zone;

As discussed is the previous section, virtual faults are then modelled around each hypocenter if the selected GMPE require finite-fault distance metrics. Note that the top of the rupture of the virtual fault can eventually extend at shallower depth than the minimum hypocentral depth and can reach the surface.

3.1.3 Magnitude-frequency distributions

The earthquake recurrence is described by MFDs based on a doubly truncated exponential distribution (Gutenberg and Richter 1956). The calculation of Gutenberg–Richter (G–R) parameters is performed using the Weichert (1980) maximum likelihood approach. The uncertainties in the G–R parameters a and b for each zone is quantified by directly propagating the uncertainties on earthquake catalogue in terms of earthquake magnitude and completeness period via Monte Carlo approach. In practice, for each zone, 200 synthetic catalogues are generated by sampling uncertainties on Mw and completeness periods and for each realization a G–R model is fitted (using the maximum likelihood method) to the calculated rates. The synthetic catalogues are generated by sampling the uncertainties distributions considering truncated normal distributions (truncation at 1 sigma).

The uncertainties of the catalogue Mw values are defined for historical events in the SIGMA catalogue (Manchuel et al. 2017) based, for example, on the quality of the macroseismic data and reliability of depth estimation for the historical events. For the events of the SIGMA catalogue belonging to the SI-Hex catalogue a generic uncertainty value of 0.2 magnitude unit is used representing a typical uncertainty value associated to magnitude conversion equations. The uncertainties on the completeness period for the different magnitude classes were already presented in Table 1.

An example of the outputs of this approach is presented in Figs. 3 and 4 for zone 4007 of SM3 and zone CBD of the SM1 area source models, respectively. These two zones present different geographical extents and are characterized by a significantly different rate of earthquakes. Therefore, the MFDs are characterized by quite different uncertainties. We can also note the strong correlation (close to 1 in both cases) of a and b values obtained by this procedure. Such correlated a and b values are directly propagated into the SSC logic tree avoiding unrealistic activity rates that may results from the use of MFD obtained by propagating the uncertainties in a and b values in an uncorrelated way. The epsilon$_b$ = $(b - \mu_b)/\sigma_b$ and epsilon$_a$ = $(a - \mu_a)/\sigma_a$ values are modeled as correlated normal distributions. For each area source, 100 epsilon$_b$ values are sampled from the normal distribution and, for each value, the conditional value of epsilon$_a$ is calculated based on the correlation coefficient and its uncertainty.

The distributions of a and b values obtained for each zone of the three area source models considered in this study are illustrated in Fig. 5. The a values (normalized to 10^6 km^2) mostly range between a = 3.5 and a = 4.5 as typically observed for zones of low seismic activity (Johnston et al. 1994 obtained a = 3.458 from a global catalogue of stable continental regions). Values exceeding a = 4.5 are observed in the most active
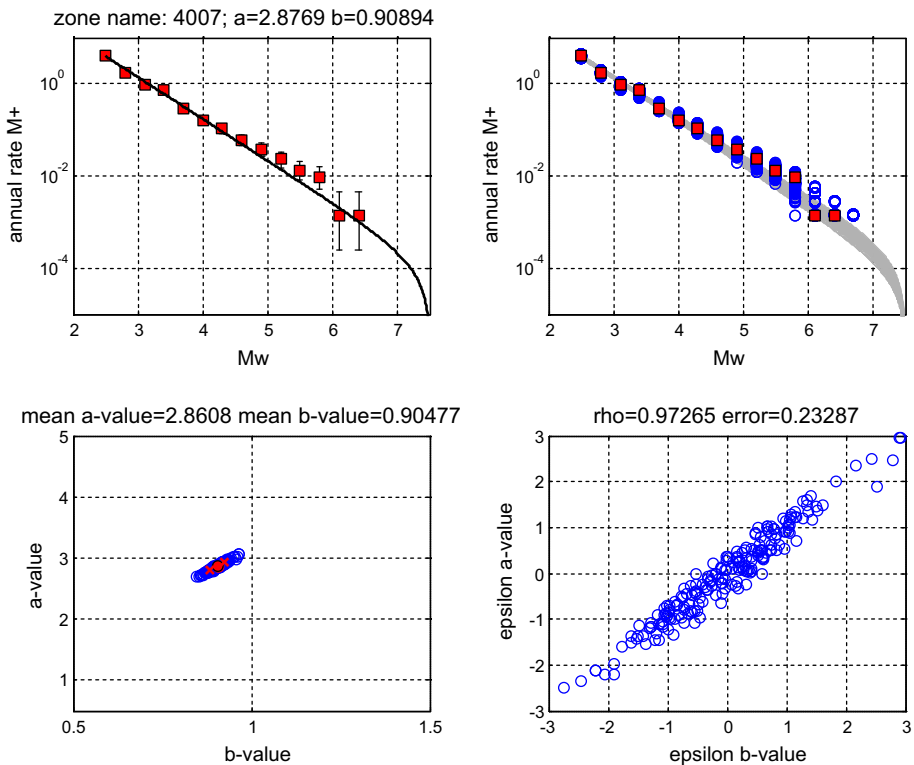
Fig. 3 Magnitude-frequency distribution and G-R parameters for zone 4007 of SM3. Upper-left: G-R derived based on the observed rates in the catalogue. Vertical bars represent the 16–84 confidence intervals. Upper-right: G-R models (in gray) derived from 200 synthetic catalogues. Blue circles represent the rates for each synthetic catalogue and red symbols the observed rate for the initial catalogue. Lower-left: a and b values of the 200 G-R models (blue circles) the mean, 16 and 84 percentiles are represented by red symbols. Lower-right: correlation (rho) and root mean square error of $epsilon_b = (b-\mu_b)/\sigma_b$ versus $epsilon_a = (a-\mu_a)/\sigma_a$

zones of the Alps. The b-values show some variability among the source zones, which is the result of the adopted procedure that aims to exploit as much as possible the seismicity data within each zone. Anyway most of the b-values ranges between 0.8 and 1.1 and do not exceed the range 0.7–1.2 in agreement with global estimates (Schorlemmer et al. 2005). Finally, we may observe that the fluctuations of a and b values among the source zones appear clearly correlated.

The parameters of the MFDs used in the PSHA calculations are reported in the Electronic supplement to this paper.

3.2 Maximum magnitude distribution

The maximum magnitude (Mmax) is the magnitude of the largest earthquake thought to be possible within a specified area, or source zone. This parameter is required in PSHA to avoid including in hazard calculations earthquakes that would be unrealistic, given the seismotectonic context. Different methodologies may be applied to assess the Mmax (see Wheeler 2009) but regardless of the different available approaches, the determination of
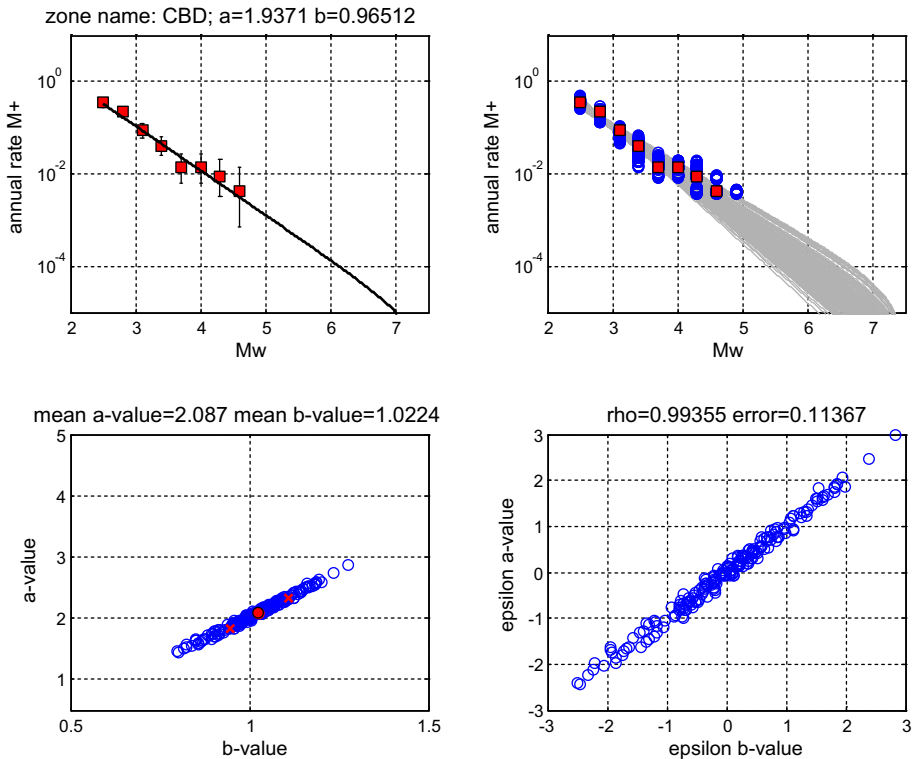
Fig. 4 The same as Fig. 3 but for zone CBD of SM1

maximum earthquake magnitude remains significantly uncertain, and this uncertainty needs to be addressed. In this project, the Mmax distributions are derived from a Bayesian approach, inspired by the Johnston et al. (1994) approach, and adapted to the French context as discussed in Ameri et al. (2015). We recall here that the approach relies on the definition of two priors Mmax distributions based on the maximum observed magnitudes over large aggregations of zones (super-domains) at European level. Ameri et al. (2015) defined two priors: one for the more active regions (French Alps and Pyrenees) and one for the less active regions of France. These prior distributions are then updated in the Bayesian framework by calculating likelihood functions using the earthquake catalogue developed for this study. In order to calculate the likelihood functions using a statistically significant number of events, several domains are defined covering the French metropolitan territory. Then posterior Mmax distributions are proposed for each of these domains. Three Mmax domains are of interest for this study, covering the southeastern France: the active domain of the Alps, the intermediate domain of the South-East, and the intermediate domain of the Central Massif (Fig. 6). For the first domain, the prior Mmax distribution for the French Alps is used whereas for the remaining domains we used the prior for less active areas. In the PSHA calculations, a Mmax distribution is associated to each zone of the AS models according to its location in one of the three domains. Note that despite the quite different geometries of the considered AS models, the boundaries between the three domains are largely consistent with zones boundaries in the three AS models, confirming that the boundaries of the domains corresponds to major seismotectonic limits. This results in a
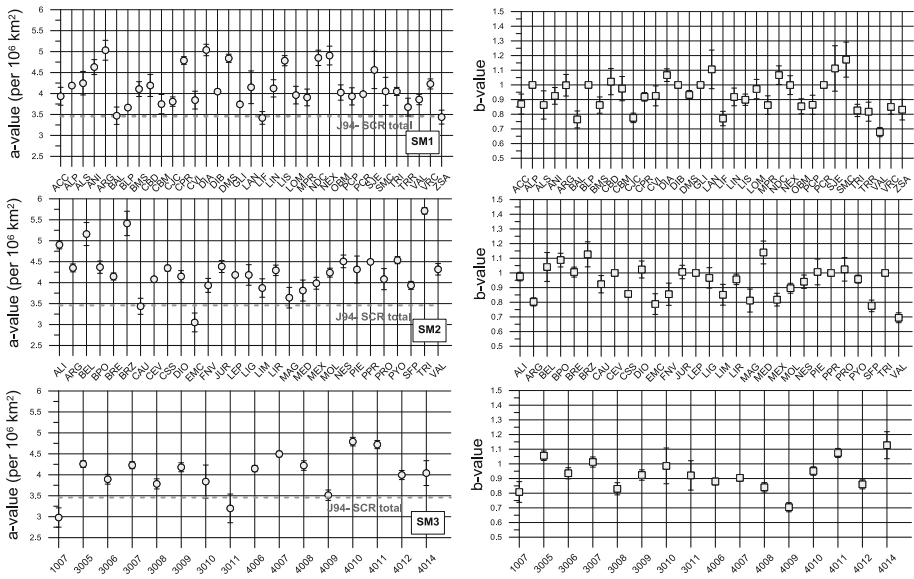
Fig. 5 Left: mean a values (normalized to 10^6 km^2) and relative standard deviations obtained for the zones of the area source models SM1 (top), SM2 (middle), SM3 (bottom). The horizontal dashed line mark the a value obtained by Johnston et al. (1994) for stable continental regions (SCR-Total). Right: mean b values and relative standard deviations obtained for the zones of the area source models SM1 (top), SM2 (middle), SM3 (bottom)

good spatial consistency of Mmax distributions among the three AS models. The Mmax distributions used for the zones belonging to the three domains are presented in (Fig. 7). The Mmax distributions are approximated by a five-point distribution and 100 Mmax samples are drawn from the distribution and combined with a and b values to model the MFDs.

Since the area source TRI of model SM2 is a very small zone conceived to include the peculiar seismic activity of the Tricastin area characterized by very shallow events, the Mmax is limited to 5.5 due the to the maximum fault dimension that can be contained by the zone.

3.3 Smoothed seismicity models

As an alternative to the AS models presented above, a smoothed seismicity model is included in the SSC logic tree based on the activity rates observed in the declustered earthquake catalogue. The smoothed seismicity approach compared to the area sources provides a representation of the seismicity rate in the study area that is not affected by the sometimes subjective and debatable delimitation of the zone boundaries. The smoothed rates are mostly controlled by the earthquake catalogue and by the choice of the smoothing kernels. The smoothed seismicity model is described by a grid of point sources whose MFDs correspond to a double truncated GR. We used 2-D, isotropic, Gaussian smoothing kernels with spatially adaptive radii according to Helmstetter et al. (2007). The smoothing width at a given point is equal to the distance to the *n*th closest earthquake with Mw equal to or greater than a minimum magnitude threshold and therefore it is density dependent. In highly active areas, the smoothing width is thus much shorter than in weakly active areas.
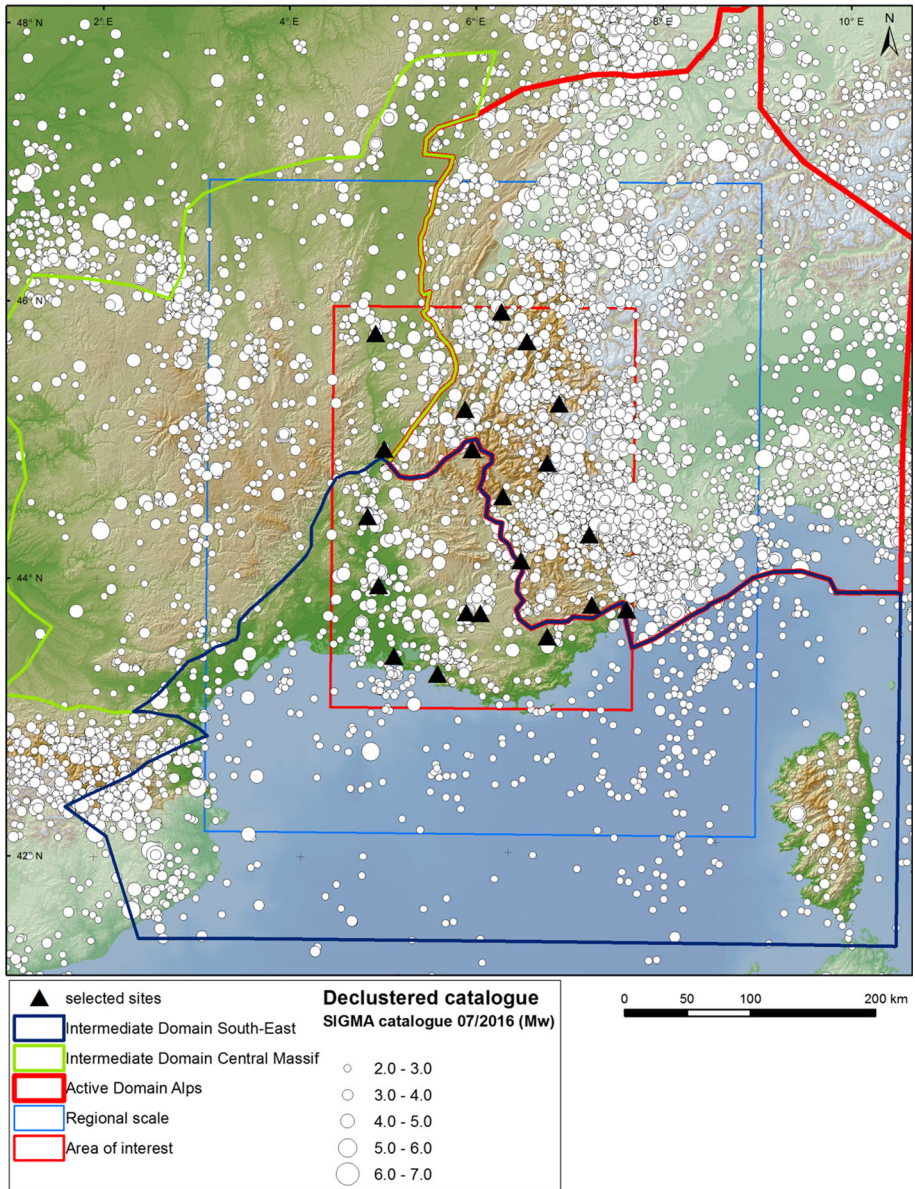
Fig. 6 Map of the three Mmax domains covering Southeastern France. The declustered earthquake catalogue used in this study and the target sites (black triangles) are reported on the map

For this study, we used two kernels characterized by 5th nearest neighbors (named SA05_MXP) and 20th nearest neighbors (named SA20_MXP). In the first case, the smoothed rate is representative of the seismicity observed locally while in the second case, the smoothing distance width is larger and the rate depends on a larger set of earthquakes.

The seismicity rates are calculated from a declustered earthquake catalogue using only the data within the completeness periods. The completeness period obtained for low-
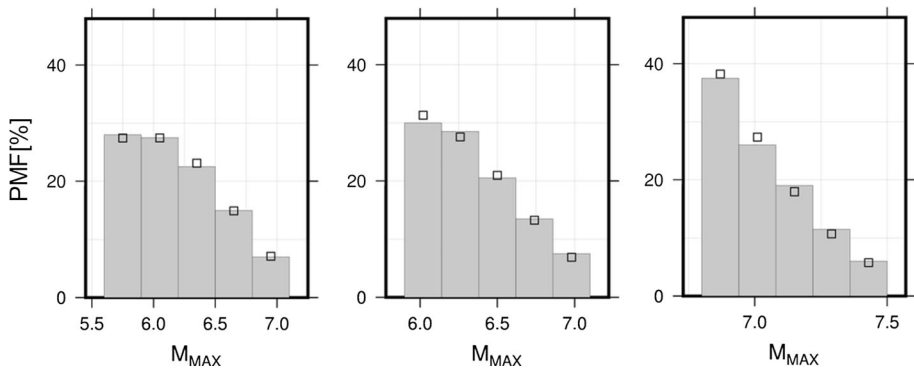
Fig. 7 Mmax probability mass function (PMF) used for the zones belonging to the intermediate domain of the South-East (left), intermediate domain of the Central Massif (center) and active domain of the French Alps (right).Histograms represent the distribution of the 100 Mmax samples used in the calculation. The open squares represent the theoretical PMF from the Bayesian approach

population density area is used for conservatism (see Table 1), and because the use of two completeness periods regions is not applicable at this stage. The smoothed gridded seismicity rates calculated at each Mw bin are analyzed to evaluate the Gutenberg-Richter parameters at each grid point using the maximum likelihood approach (MXP) for a fixed b-value equal to 1.0. A minimum magnitude Mw $= 3$ is used for the GR calculation which is consistent with the values used for the AS models. Note that the uncertainties in the GR parameters are not formally considered in the smoothing approach. The uncertainties obtained with the maximum likelihood approach are indeed quite small due to the large number of events available at each grid point. Instead of propagating such uncertainties in the calculations with a large penalty for the computational time and complexity of the model, we preferred to use alternative smoothing kernels, which in some sense account for uncertainties in activity rates. In order to assign Mmax, depth distribution and faulting mechanism to each grid point and to constrain spatially the smoothed seismicity, we considered the super-domains identified in the previous section. The Mmax distributions presented in Fig. 7 are used for the MFDs of each grid point according to their association to each domain. The fault mechanisms are defined as follows:

- Strike-slip (weight $= 0.7$) and reverse (weight $= 0.3$) for the French Alps domain;
- Strike-slip (weight $= 0.7$) and normal (weight $= 0.3$). for the other two domains.

The sources hypocentral depths are between 5–20 km (i.e., epistemic uncertainties are not considered for the smoothed seismicity model) and the aleatory distribution of focal depths within the seismogenic layer is the same as defined for area source models. As for the AS models, virtual faults are generated for each grid point in order to calculate all the necessary distance metrics for the GMPEs. The parameters for the virtual faults are the same used for the AS models. Finally, the boundaries of the three domains are treated as strict or leaky as epistemic uncertainties in the logic tree. This means that, in case of strict boundaries, the width of smoothing kernel is bounded by the domains limits. Figure 8 shows the smoothed a-values in the study region considering SA05_MXP and SA20_MXP kernels for leaky and strict boundary conditions of the domains. In case of SA05_MXP smoothing kernel, the spatial distribution of the activity rates (a values) follows much closer the actual distribution of seismicity, than for SA20_MXP where the activity is more
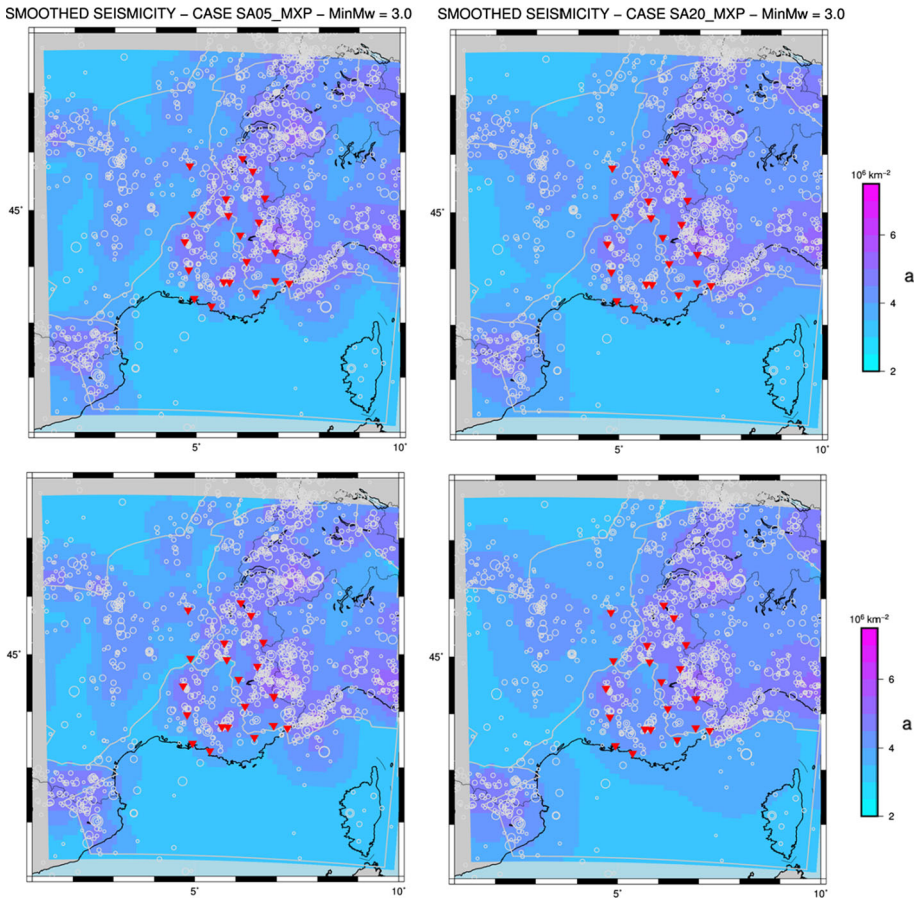
Fig. 8 Map of smoothed a-values (normalized to 10^6 km^2) for the SA05_MXP (left) and SA20_MXP (right) kernels considering leaky (top) and strict (bottom) boundaries

spatially smoothed. We also clearly observe the effect of the leaky versus strict boundary conditions, more evident for the SA20_MXP kernel. For example note the change in the smoothed rates offshore of Nice and along the Ligurian coast, close to Valence and more in general along the border of the domains.

3.4 Fault Sources

The use of fault models is strictly related to the level of knowledge on the active structures in the target area. When the information on identified faults is sufficient and robust enough to allow the parametrization of fault models (geometry, slip rates), then such models can be introduced in the PSHA as fault sources. No published active faults database exists in France and the work package 1 of the SIGMA project was partially devoted to the investigation of active faults in the French area. Despite these efforts, the characterization of active faults in the target area is still affected by large uncertainties that prevent the development of fault models for the entire region. These uncertainties concern the faults geometries and mostly the quantification of the slip rates. The only notable exception is

represented by the Middle Durance Fault (MDF), that is probably the best investigated structure in France (Cushing et al. 2007), and the surrounding compressive structures of Provence. Recent works by Guyonnet-Benaize (2011) and Guyonnet-Benaize et al. (2015) provided a three-dimensional geological model of the deep basin structure of the Middle Durance region by integrating geological and geophysical data in a unique modeling environment. After discussion within the SSC team and with the SIGMA scientific committee, it was decided to include the faults of the Provence region in the SSC logic tree.

The fault model is presented in Fig. 9 according to the geometry and segmentation by Guyonnet-Benaize et al. (2015). The fault model is combined with the area source model SM1 in order to model the seismic activity in areas not covered by the faults. In the zone encompassing the faults (PCP), the background seismic activity is limited to Mmax = 5.9 (i.e., smaller than the minimum characteristic magnitude considered on the faults) and earthquakes with Mw ≥ 6 are assumed to occur only on faults. The parameters characterizing the fault segments in terms of geometry, activity, and kinematic are defined in Table 2.

In the hazard calculations, the hypocenter location is randomly sampled on the fault. For each magnitude scenario, the rupture area and fault aspect ratio are defined according to the Wells & Coppersmith (1994) empirical scaling relation. The epistemic uncertainty associated to the fault geometry (namely the dip and width of the various sub-segments in this case) is not considered in this study. The recurrence of earthquakes on the faults is described by the Youngs and Coppersmith (1985) characteristic model with parameters as reported in Table 2. The M_{char} is assumed as the central value between Mw = 6 (i.e., the minimum magnitude on faults) and the Mmax for each fault segment. The Mmax is determined based on several empirical scaling relations (Leonard 2010; Papazachos et al.
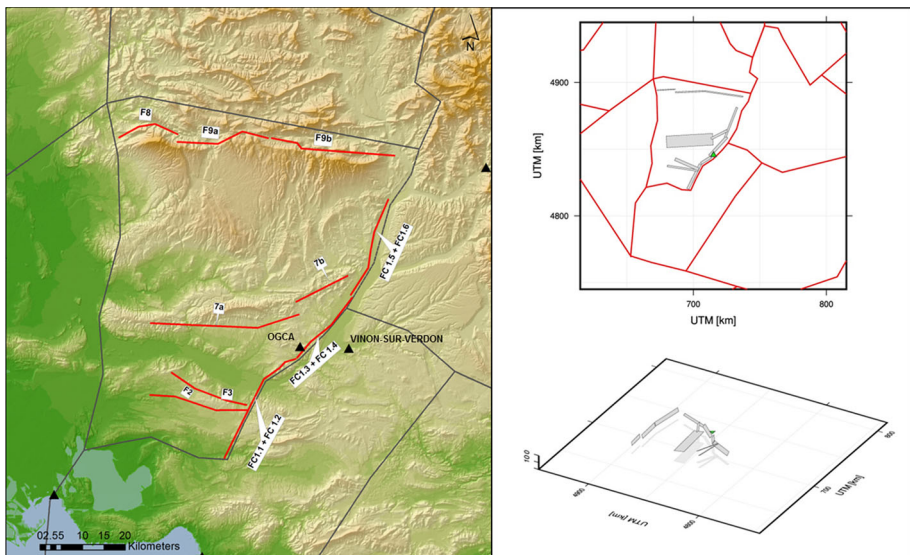

Fig. 9 Left: map of the surface traces of fault segments considered in the model (in red). The background zone of the fault model is zone PCP of SM1. Right: representation of the simplified fault model as implemented in the PSHA. Top: map view; Bottom: view from south-west. Grey rectangles represent the fault plane of the different fault segments. The green triangle represents the OGCA site, which is the closest of the considered target sites to the fault model

Table 2 Summary of fault source characteristics included in the SSC model

name	Segment	Style of faulting	Length (km)	Hypocentral Depth (km) [min–max]	Slip rate (mm/year) [min–max]	Mean Dip (°)	M_{char}	ΔM_{char}
Trévaresse	F2	Reverse	24	2–3	0.050–0.30	38	6.3	0.30
Costes- Trévaresse	F3	Reverse	22	2–4	0.010–0.07	43	6.3	0.30
Grand Luberon	F7a	Reverse	35	3–5	0.002–0.03	13	6.5	0.50
Manosque Fold	F7b	Reverse	13	2–5	0.002–0.03	60	6.1	0.10
Ventoux Thrust	F8	Reverse	15	3–8	0.002–0.03	85	6.1	0.10
West-Lure Thrust	F9a	Reverse	24	3–8	0.002–0.03	80	6.3	0.30
East-Lure Thrust	F9b	Reverse	30	3–8	0.002–0.03	80	6.4	0.40
Middle Durance Fault	FC1.1 + FC1.2	Strike-slip	29	2–7	0.010–0.10	70	6.35	0.35
Middle Durance Fault	FC1.3 + FC1.4	Strike-slip	18	3–6	0.010–0.10	56	6.25	0.25
Middle Durance Fault	FC1.5 + FC1.6	Strike-slip	23	4–6	0.010–0.10	56	6.30	0.30

2004; Wesnousky 2008) as a function of rupture length, rupture area and fault mechanism of each segment. ΔM_{char} is defined as Mmax-M_{char} for each segment.

3.5 SSC logic-tree

In this section, we summarize the characteristics of the SSC logic tree that is composed by the elements described so far in this paper. The two main branches are a model-based source description and a smoothed seismicity source description (Fig. 10). Model-based seismicity is described by the three area source models (SM1, SM2 and SM3) and a fault model + background zones (called SM1'). The smoothed seismicity considers different boundary conditions of the three domains (i.e., leaky or strict) and different parameter of the smoothing kernel.

The distributions of the Mmax for the AS models and smoothed seismicity models have been described in Sect. 3.4. The approach followed to propagate the uncertainties in the MFDs for the AS models has been discussed in Sect. 3.1.3. The uncertainties on the slip rate for the fault model are propagated assuming a uniform distribution to characterize the uncertainties between the lower and upper bound slip rates (Table 2).

Concerning the logic-tree weights, following the discussion within the project team, the recommendations of the SIGMA scientific committee members and recent outcomes from the SHARE project (Woessner et al. 2015) it was decided to use different weights depending on the return period of interest. The rationale behind this choice is that for long
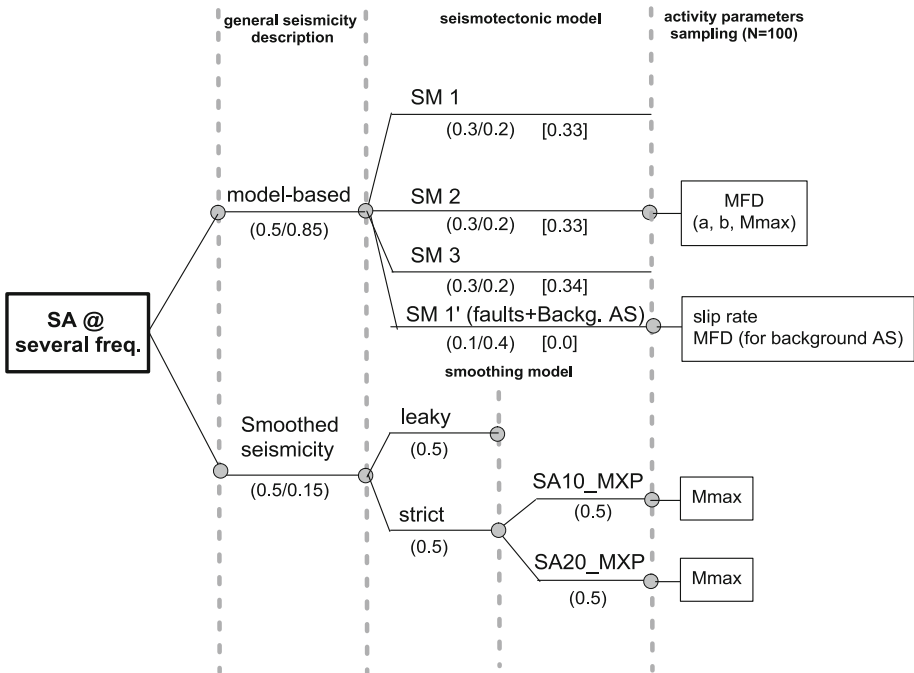

Fig. 10 SSC logic tree considered in this study. The numbers in brackets are the weights assigned to each branch. Multiple numbers represent different weights for 475 yrs and 10,000 yrs return periods. Numbers in square brackets are the weights for sites where the fault model is not considered

return periods (e.g., 10,000 years) our degree of belief on the smoothed seismicity model based on the observed seismicity over a relatively short time period is smaller than on AS and fault models. For short return period (i.e., 475 years) equal weight is given to model-based and smoothed seismicity whereas at long return periods (i.e., 10,000 years) larger weight is given to model-based seismicity. Moreover, the weights depend also on the target site because the fault model affects only two sites (OGCA and Vinon-sur-Verdon) and thus faults are not considered for the other sites (zero weight is assigned). Among the AS models, for sites not affected by the fault model, equal weights are given to SM1, SM2 and SM3, regardless the return period. For the sites affected by the fault model, at 475 years return period a smaller weight is given to the fault model (0.1) compared to the area source models. On the contrary, at 10,000 years return period the fault model has larger weight (0.4).

4 Ground motion characterization (GMC)

The characterization of the ground motion in metropolitan France was clearly a major challenge of the work package 2 of the SIGMA project. Southeastern France is characterized by a low-to-moderate seismicity and consequently the available strong-motion records are very limited in the magnitude/distance range of interest for seismic hazard assessment. As a result, seismic hazard assessment in France is typically performed using GMPEs derived from data collected in other regions. Beauval et al. (2012) tested a number of these GMPEs against French strong-motion records and found that the best-fitting models over the whole frequency range are the Cauzzi and Faccioli (2008), Akkar and Bommer (2010), and Abrahamson and Silva (2008) models. However, these models are now superseded by more recent versions based on updated and augmented databases and functional forms.

Within the SIGMA project, a major effort was the construction of the RESORCE database (http://www.resorce-portal.eu/), that contains strong-motion recordings for the Pan-European region, designed for the testing of existing GMPEs and the development of new ones. Based on RESORCE, several new models have been produced (see Douglas et al. 2014a). However, although being based on European data, these GMPEs do not consider French records. For this reason, within the WP2, two GMPEs have been developed for a better ground motion characterization in France: the empirical model by Ameri (2014) (updated by Ameri et al. 2017a) and the stochastic model by Drouet and Cotton (2015).

In this study, the set of GMPEs is selected by combining the models developed within the SIGMA project with recent models for the Pan-European region and for global datasets. GMPEs from global datasets are selected in order to have a better constrain of ground motions for large magnitudes. Note that, Campbell (2016) indicated that the quadratic magnitude scaling function used by many of the Pan-European GMPEs (and also by Cauzzi et al. 2015) might not have enough flexibility to capture the data trends, particularly in the mid magnitude range which is important for the French context. The main characteristics of the selected models are listed in Table 3. Note, that the selected GMPE comply with the criteria proposed by Cotton et al. (2006).

Among the GMPEs from the NGA-west 2 project, the model by Boore et al. (2014) is considered because its relatively simple functional form (compared to the other NGA-west 2 GMPEs) is judged more appropriate to the adopted SSC logic tree mostly composed by

Table 3 Main characteristics of selected GMPEs for the GMC logic tree

GMPE	Region (dataset)	Mw range	Distance range	Period range	Site	Fault mechanism
Ameri (2014)	Europe -middle East + French and Swiss data	Mw = 3.0–7.6	$R_{JB,EPI}$ = 0–200 km	PGA; 0.01–3 s	4 site classes	Yes
Drouet and Cotton (2015)	French data (Stochastic model)	Mw = 3–8	R_{EPI} = 1–250 km	0.01 and 3 s	Rock or hard rock	No
Akkar et al. (2014)	Europe -middle East	Mw = 4.0–7.6	$R_{JB,EPI, HYP}$ = 0–200 km	PGA; 0.01–4 s	Vs30	Yes
Bindi et al. (2014)	Europe -middle East	Mw = 4.0–7.6	$R_{JB,HYP}$ = 0–300 km	PGA; 0.02–3 s	vS30 or site classes	Yes
Boore et al. (2014)	Global (mostly California)	Mw = 3.5–8.5	R_{JB} = 0–400 km	PGA; 0.01–10 s	vS30	Yes
Cauzzi et al. (2015)	Global (mostly Japanese)	Mw = 4.5–7.9	R_{RUP} = 0–150 km	PGA; 0.01–10 s	vS30 or site classes	Yes

area sources. Indeed, other NGA-west2 GMPEs contain a number of parameters that are difficult to constrain in the modeling of area sources in low-seismicity zones. The use of default values for these parameters could lead, however, to underestimate the overall aleatory variability of the models (Bindi et al. 2017).

The selected set of GMPEs attempts to capture, to the extent possible, the epistemic uncertainties in the regional ground motion characteristics for the target area. At the same time, we aim to limit the number of GMPEs to models that are mutually exclusive. We recognize that the Akkar et al. (2014) and Bindi et al. (2014) models share the same dataset and we consider this issue in the assignment of logic tree weights as discussed in the following of the paper.

4.1 GMC logic tree weights

For the return periods of interest for this study (i.e., 475 years and 10'000 years), the hazard deaggregation performed on a preliminary logic tree for test sites clearly indicated that the largest contribution to the hazard comes from Mw below 6.5. For this magnitude range, all the selected GMPEs are well constrained because the datasets are relatively abundant of records. However, the sample of records from events in the target area available in the RESORCE database is too small and limited to attempt any GMPE testing that would help to assign weights in a more quantitative way. Moreover, a model ranking good considering small magnitude events does not necessarily mean a similar performance for large magnitudes. Therefore, the set of logic tree weights is based on the following simple and transparent arguments (Fig. 11):

- The first criterion is based on the use of data from the target area (French Alps). The models are separated in two sets depending on the use of French data. A weight w = 0.5, is given to set of two GMPEs that consider data from the area of interest (Drouet and Cotton 2015 and Ameri 2014) and a weight w = 0.5 is given to the set of GMPEs that were derived without considering French strong-motion recordings.
- A second criterion, applied only to the set of GMPEs that do not consider French data, is based on the similarity of the underlying datasets used for GMPEs derivation. Akkar et al. (2014) and Bindi et al. (2014) use similar datasets and a weight w = 0.3 is given to the ensemble of these two GMPEs. Cauzzi et al. (2015) and Boore et al. (2014) consider datasets that are largely independent and weights w = 0.4 and w = 0.3 are
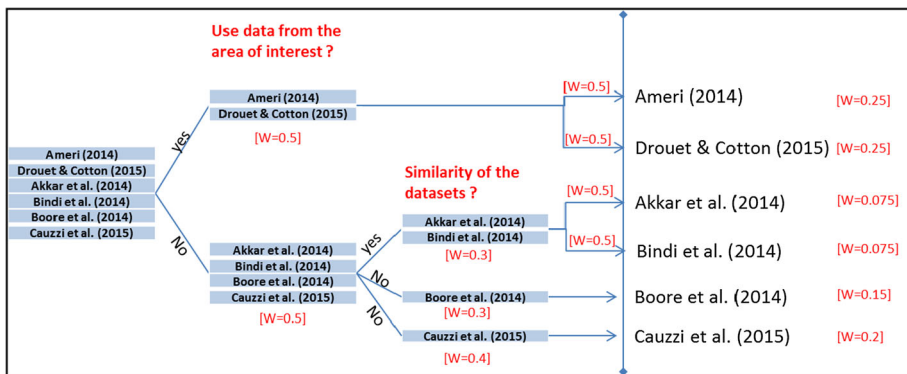
Fig. 11 GMPEs weighting scheme considered in this study

assigned to these two GMPEs, respectively. The larger weight assigned to the Cauzzi et al. (2015) model is due to their use of a completely digital-records dataset.

- Finally, equal weights are assigned between the Drouet & Cotton (2015) and the Ameri (2014) GMPEs and between the Akkar et al. (2014) and Bindi et al. (2014) GMPEs.

The final weights of the GMPEs are reported in Fig. 11.

5 Results

The software used to perform the PSH calculations is the *SHA_Toolbox* software, a in-house PSHA code developed under QA process. The *SHA_Toolbox* is able to handle complex logic trees and to propagate in a complete and appropriate way both aleatory and epistemic uncertainties. The *SHA_Toolbox* is regularly submitted to extensive verification and validation (e.g. PEER tests by Thomas et al. 2010 and analytical solutions for canonical models) and it is applied to nuclear studies and complex tectonic environments.

A minimum magnitude of Mw = 4.5 is used in the PSHA calculations. The results are presented in terms of mean and percentile (16, 50 and 85th) uniform hazard spectra (UHS) at 475 years and 10,000 years return periods for the 20 considered sites (Fig. 1). A generic rock condition characterized by a Vs30 = 800 m/s or equivalent site class is considered.

5.1 Results of the present study

The hazard results are presented for the 20 sites at two return periods (475 and 10,000 years) in Fig. 12. The mean and 16, 50 and 84th percentiles PGA and spectral acceleration at 1 s are shown in order to compare the hazard levels over the considered region. In Fig. 12 the sites are generally ordered according to the seismic activity of their zone. Sites located in the active domain of the Alps are placed in the upper part of the figure, while sites located in the intermediate domains are the bottom. As expected, we observe an increase of the estimated acceleration values moving from the intermediate activity domains toward the more active domain of the Alps. In order to compare the hazard distribution between different sites, an uncertainty metric is calculated as: $100*\log(PSA_{84}/PSA_{16})$, where PSA_{84} and PSA_{16} are the 84th and 16th percentiles spectral acceleration at a given period. Note also that these numbers are directly comparable with the values reported by Douglas et al. (2014b) for several PSHA studies worldwide. We do not observe any clear trend in the uncertainty values in the intermediate and active domains. We note however that the uncertainties at 475 yrs return period are almost systematically larger than at 10,000 yrs.

In the following, we will focus on some specific sites in order to discuss the mean UHS and the associated uncertainties (Fig. 13). As a first example, we consider Marseille and Lyon, two cities relatively far from each other, located in the intermediate activity domains with very similar mean UHS at 475 years return period and yet characterized by a substantially different uncertainty. Figure 14 presents the mean UHS at 475 years return period obtained by specific source model branches. We can clearly see how the variability given by the three AS models and smoothed seismicity models is much larger for Marseille than for Lyon. For the AS models, this is due to the variability in the geometries and the activity rates of the area sources controlling the hazard at this return period, that is larger for the zones around Marseille. Moreover, at Marseille, the UHS for the smoothed-seismicity models provide significantly lower accelerations with respect to the AS models.
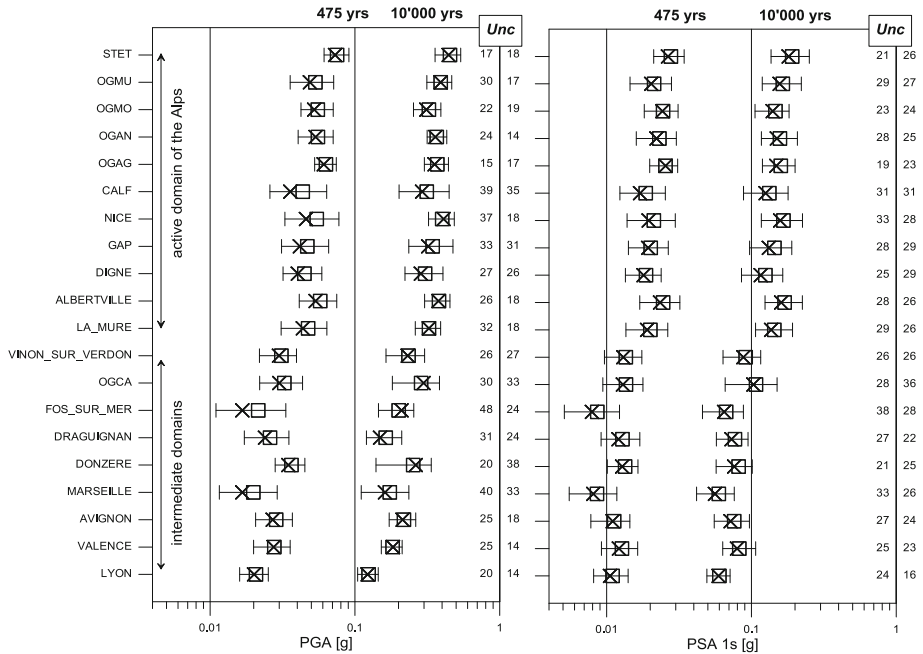
Fig. 12 PGAs (left) and spectral acceleration (PSA) at T = 1 s (right) for the 20 selected sites (Vs30 = 800 m/s) for return periods of 475 and 10,000 years (bars, 16th–84th fractiles; crosses, medians; and squares, means) and the uncertainty metric Unc = $100*\log(PSA_{84}/PSA_{16})$. The uncertainty values are for 475yrs (left) and 10,000 yrs (right) return periods

This is because the local seismic activity is relatively low is Marseille, especially offshore (to the South) whereas, the AS models extending mostly to the North, account for the higher seismic activity of the Provence region. In Fig. 14, we can also observe the difference among the smoothed seismicity models in Lyon and, particularly, between the SA_05 and SA_20 kernels. The former provides larger accelerations than the latter, particularly at high frequencies. This is due to the higher activity rates at the site provided by SA_05 kernel (Fig. 8) that being characterized by a smaller smoothing distance attributes higher rates to local seismicity close to the site (Fig. 1). Finally, the smaller uncertainties in Lyon at 10,000 years are also related, particularly at low frequency, to the smaller range on Mmax values considered in the source models (Fig. 7).

Figure 15 shows the mean UHS at 10,000 years return period obtained at OGCA site for each of the seismic source model considered in the SSC logic tree. The purpose is to show the impact of the fault model on the hazard level. The spectral accelerations obtained using the fault model (SM1') are larger than those by the AS and smoothed seismicity models. In particular, the UHS for SM1' is significantly larger than the one for SM1 which is the background area source model without including faults. This demonstrate the significant contribution of the fault model (also confirmed by hazard deaggregation by source, not shown here) and the relevance of including fault models for site located close to the faults and for long return periods. Interestingly, the UHS for SM1' is close to the one for SM2 at high frequency. We note that the zone SFP of model SM2, that controls the hazard at the site, is designed to represent the seismicity of the Provence fault systems (Fig. 2).
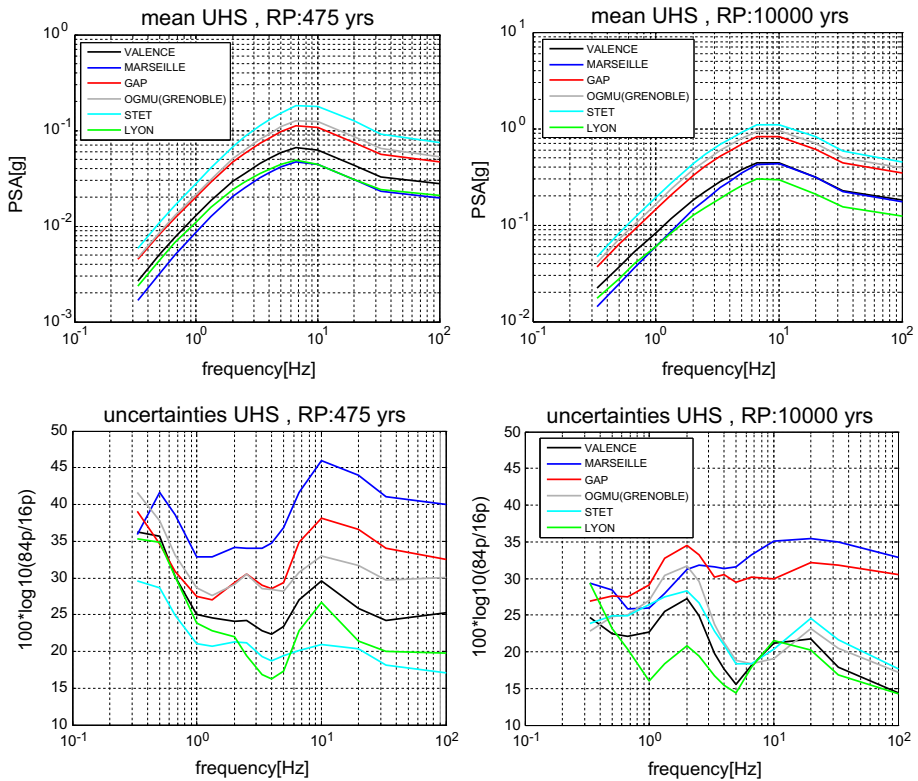
Fig. 13 Top : Mean uniform hazard spectra (UHS) for selected sites (Vs30 = 800 m/s) at 475 years (left) and 10,000 years (right) return periods. Bottom: Uncertainty metric as a function of spectral frequency for 475 years (left) and 10,000 years (right) return periods

Finally, Fig. 16 shows the mean UHS for each GMPE used in the LT for 475 years and 10,000 years return periods at Valence site. Overall, the variability of the UHS obtained by the different GMPEs is smaller with respect to what observed for the SSC model. At 475 years return period, the Cauzzi et al. (2015) model provides larger acceleration level at high frequencies with respect the other GMPEs. On the other hand, it provides lower values at low frequencies where the largest accelerations are obtained with the Drouet and Cotton (2015) model. The behavior of the Cauzzi et al. (2015) model can explain the "peak" in the uncertainty values around 10 Hz observed in Fig. 13. At 10,000 years return period, the largest acceleration values at high frequency are obtained with the Cauzzi et al. (2015) and the Drouet and Cotton (2015) models, whereas the other models provide consistently lower accelerations. At low frequencies, we observe a similar picture to the 475 years return period. Similar results are obtained for the other sites.

We point out that the larger hazard uncertainties obtained at 475 years return period compared to 10,000 years return period are mostly related to the weighting scheme adopted for the SSC logic tree branches that depends on the return period (Fig. 10). In particular, we assigned equal weights to the model-based and the smoothed-seismicity branches at short return periods. On the other hand, at long return periods much larger
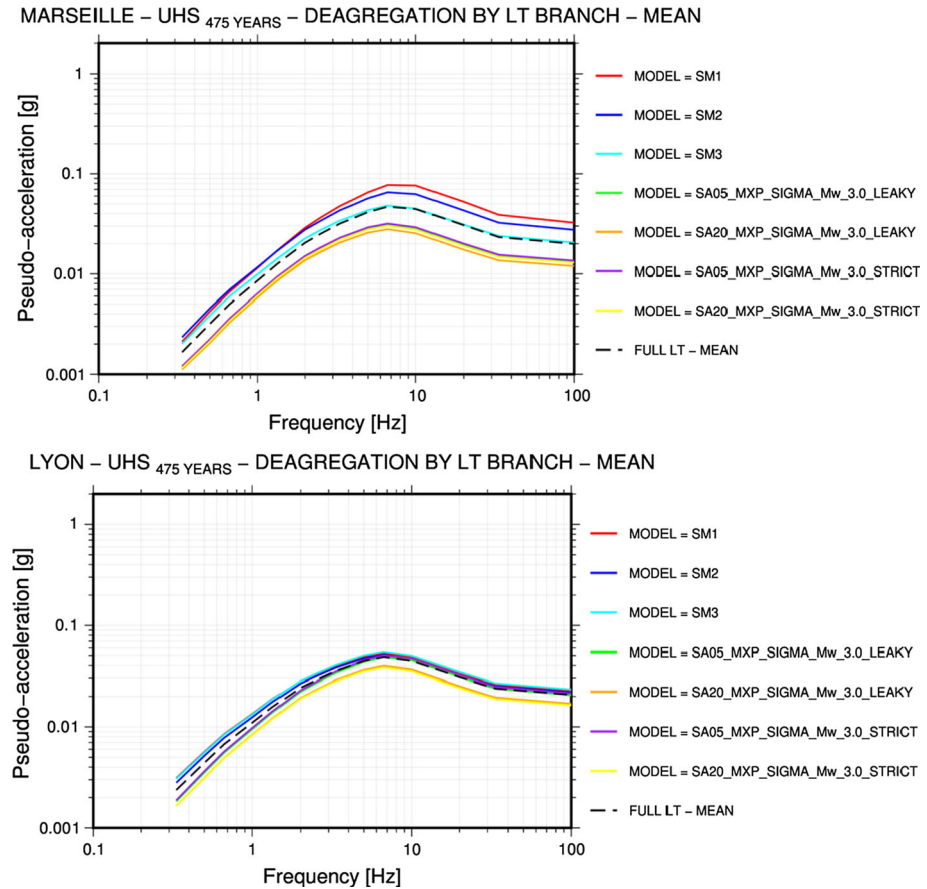
Fig. 14 Mean Uniform Hazard Spectra (UHS) for specific SSC nodes of the logic tree (LT) at 475 years return period at Marseille (top) and Lyon (Bottom) for Vs30 = 800 m/s. The mean UHS for the full LT is also shown

weight (0.85) is given to the model-based branch. This can have a strong impact on the hazard percentiles if the two branches provide significantly different hazard at the site.

The Figures showing the UHS for different percentiles and the UHS for different nodes of the logic tree for all the sites are reported in the Electronic supplement to this paper.

5.2 Comparison with previous studies

In this section, we compare the hazard results obtained in this study with those obtained in previous published PSHA studies for France. In this comparison, we consider:

- the MEDD 2002 national seismic hazard map of France project (Martin et al. 2002) that was the technical base adopted by the Ministry of Environment to develop the national seismic zonation supporting the Eurocode 8 enforcement for current buildings;
- the AFPS 2006 model (Martin and Secanell 2006) which is a refinement of the MEDD 2002 model based on the outcomes a working group of experts established by the
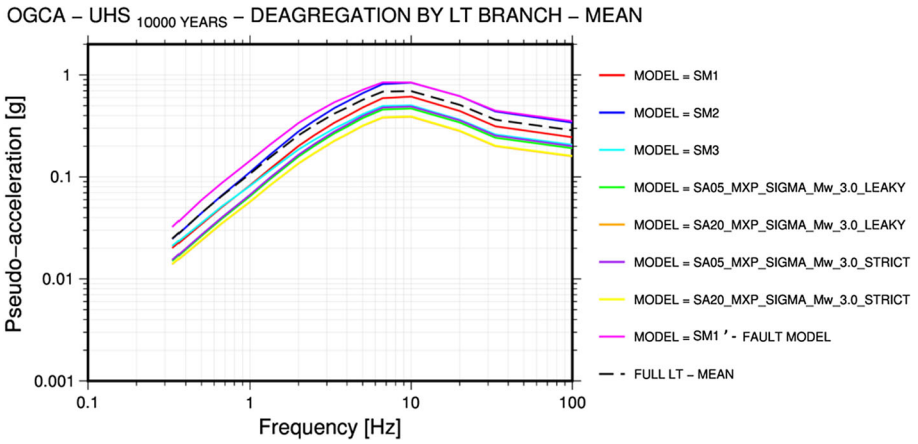
Fig. 15 Mean Uniform Hazard Spectra (UHS) for specific SSC nodes of the logic tree (LT) at 10,000 years return period for OGCA site (Vs30 = 800 m/s). The mean UHS for the full LT is also shown
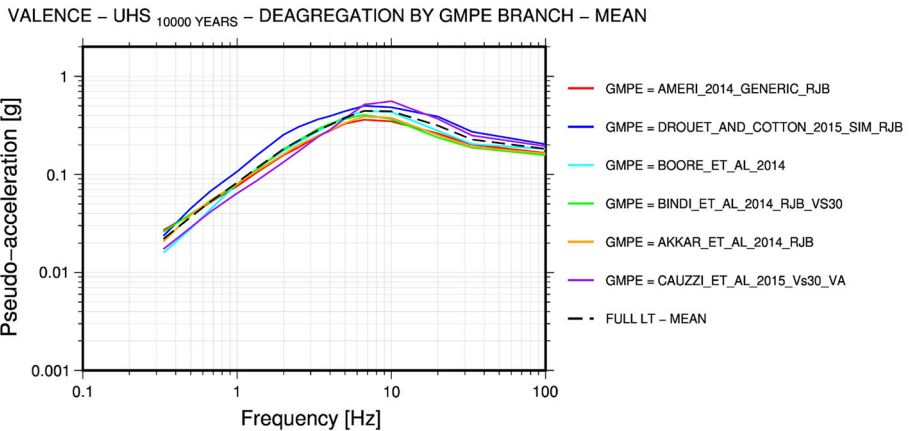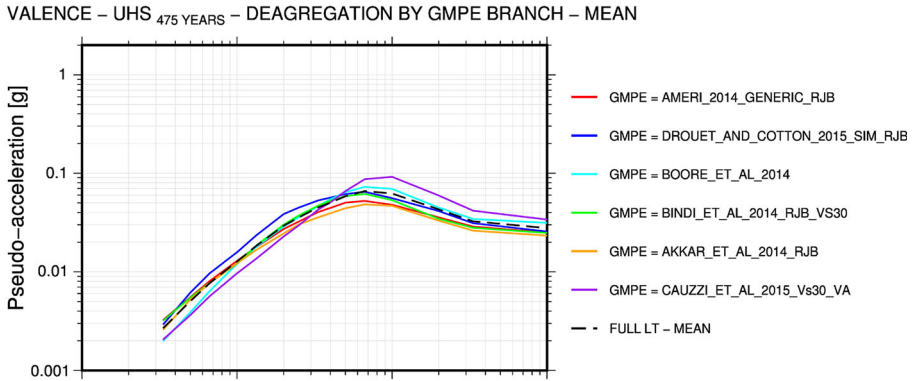

Fig. 16 Mean Uniform Hazard Spectra (UHS) for specific GMC nodes of the logic tree (LT) at 475 years (top) and 10,000 years (bottom) return periods at Valence (Vs30 = 800 m/s). The mean UHS for the full LT is also shown

French Association of Earthquake Engineering (AFPS).The results of this model were produced only in terms of PGA, and

- the 2013 European Seismic Hazard Model (ESHM13) resulting from the Seismic Hazard Harmonization in Europe (SHARE) project (Woessner et al. 2015).

We stress, that these hazard studies are based on very different hazard models and a detailed comparison of the results for the region under consideration would require an in-depth analysis of the differences in the modelling assumptions that was beyond the scope of this study. Here, we present a simple comparison of the hazard results for a specific return period pointing out possible reasons of the observed differences.

Figure 17 shows the comparison between the PGA and PSA at 1 s obtained in this study and in MEDD 2002 for a return period of 475 yrs (results for 10,000 years return period are not provided in MEDD 2002). The comparison clearly shows that at all the selected sites the accelerations by the MEDD 2002 study are systematically larger. There are several reasons for such differences, the most important being 1) the assumption of $M_L = M_S$ in the earthquake catalogue in MEDD 2002 and 2) the use of two GMPEs (Berge-Thierry et al. 2003 and Ambraseys et al. 1996) defined in terms of M_S and nowadays considered superseded by more reliable models. These two GMPEs are also based on very similar datasets and their use do not account adequately for the epistemic uncertainties in the estimated ground motions. The limitations in the ground motion model also clearly affect, the uncertainties in the hazard estimates provided in the MEDD02 study. Despite the fact that the 25th–75th fractiles are considered in the MEDD02 results (instead of the 16th–84th fractiles in this study), the MEDD02 results clearly provide very small uncertainties that are not consistent with what is observed in typical modern PSHA studies (Douglas et al. 2014a). It is then clear that the MEDD02 model cannot be considered compatible with the treatment of uncertainties and of modeling assumptions adopted in nowadays state-of-practice PSHA studies.

In Fig. 18, we present a similar comparison with the AFPS06 hazard results. In this case the comparison is performed for PGA (the AFPS06 hazard model was developed for PGA only) at the two return periods. We observe that the hazard at 475 yrs is slightly but systematically larger in the AFPS06 PSHA whereas at 10,000 years return periods the results are much more consistent. Moreover, the uncertainties in both studies are of the same order. The AFPS06 PSHA addressed several of the weaknesses of the MEDD02 model since its logic tree used a larger set of GMPEs and more appropriate magnitude conversion equations in the development of the earthquake catalogue. Moreover, expert elicitation was used to assign weights to the different branches of the GMC logic tree. On the other hand, the SSC model was essentially unchanged with respect to MEDD02. The systematic difference between AFPS06 and this study at 475 years return period is likely related to the set of GMPEs. Modern GMPEs, such as the ones used in this study, showed a clear tendency in predicting smaller acceleration values around Mw from 4 to 5 (e.g., Campbell and Bozorgnia 2014) controlling the hazard at short return periods. This is because modern GMPEs are based on datasets that extend down to small magnitudes (i.e., Mw = 3 or 4) with a better constrain on magnitude scaling and providing smaller ground motions for moderate magnitudes (Bommer et al. 2007).

Figure 19 shows the comparison between the PGA and PSA at 1 s obtained in this study and in ESHM13. In this case, for both the spectral ordinates considered we observe systematically larger values in the ESHM13 compared to this study. The use of different sets of GMPEs plays certainly an important role in the differences between the two models at 475 years. In ESHM13, two GMC logic trees are used for France one for active shallow
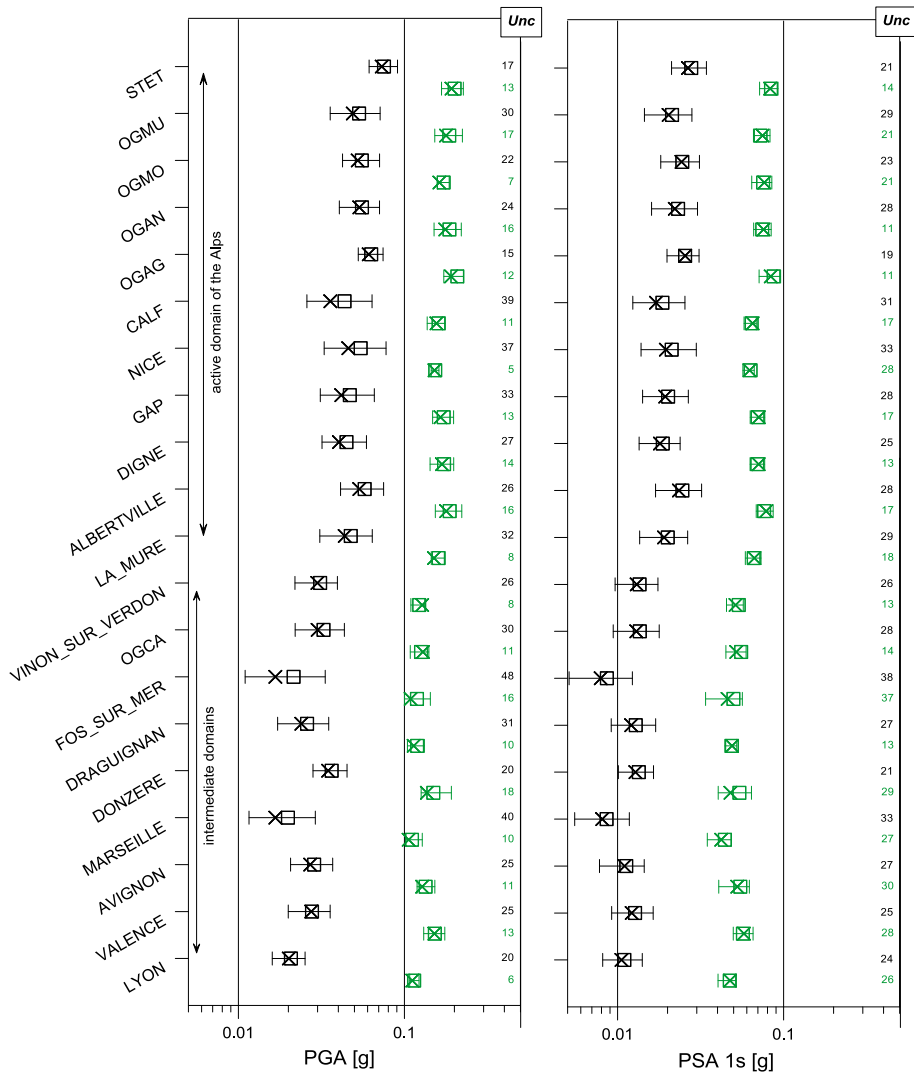
Fig. 17 Comparison of PGAs (left) and spectral accelerations (PSA) at T = 1 s (right) obtained in this study (in black) and in the MEED 2002 project (in green: bars, 16th–84th fractiles; crosses, medians; and squares, means). Results are for the 20 selected sites for return periods of 475 and generic rock conditions (Vs30 = 800 m/s). The uncertainty metric Unc = 100*log(PSA$_{84}$/PSA$_{16}$) is shown by numbers in the left vertical axis. Note that for the MEDD2002 model the 25th–75th fractiles were considered

crustal regions (ASCR) and another for stable continental regions. Southeastern France is mostly in the ASCR context and the four used GMPEs are: Akkar and Bommer (2010), Cauzzi and Faccioli (2008), Zhao et al. (2006) and Chiou and Youngs (2008). As mentioned above, more recent GMPEs provide lower accelerations for the magnitudes contributing to the hazard at 475 years return period. Another source of difference is certainly the earthquake catalogue and the procedure for the derivation of the activity rates. In ESHM13, the magnitude-frequency distributions are calculated using a relatively high
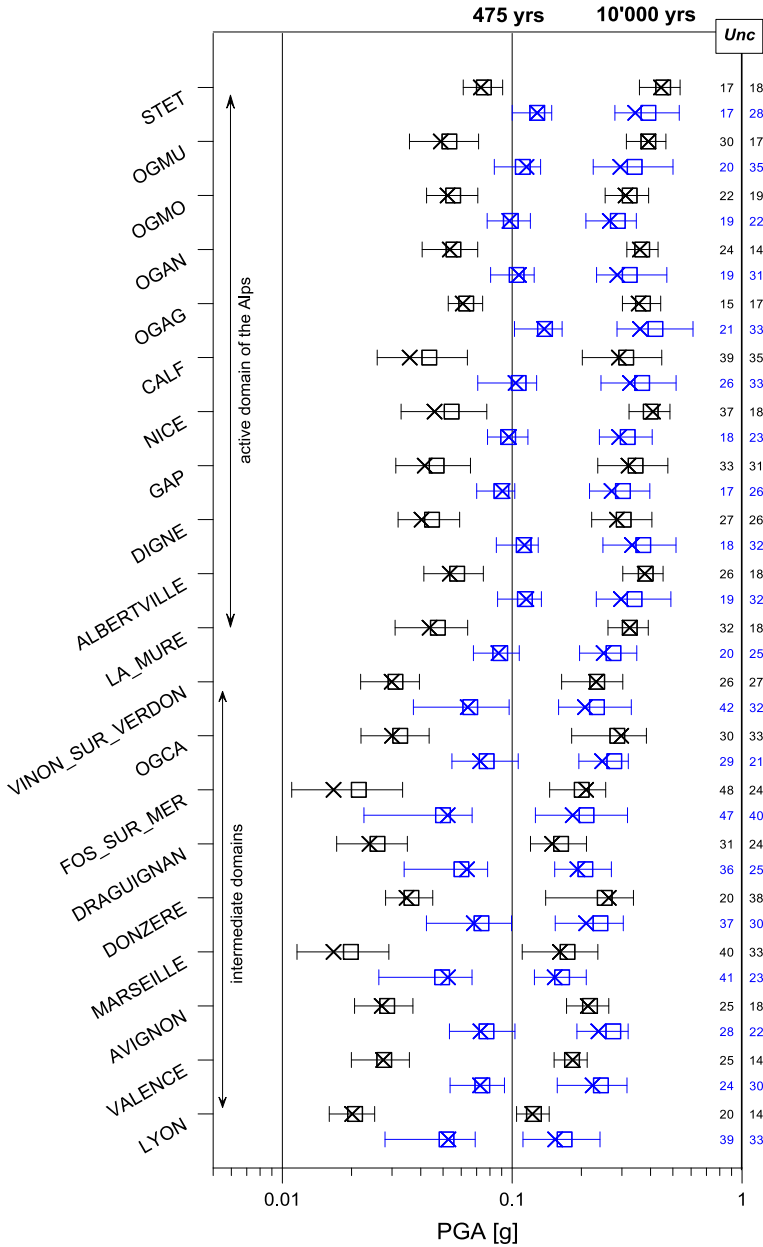
Fig. 18 Comparison of PGAs obtained in this study (in black) and in the AFPS 2006 study (in blue: bars, 15th–85th fractiles; crosses, medians; and squares, means). Results are for the 20 selected sites for return periods of 475 and 10,000 years and generic rock conditions (Vs30 = 800 m/s). The uncertainty metric Unc = 100*log(PSA$_{85}$/PSA$_{15}$) is shown by numbers in the left vertical axis. The uncertainty values are for 475yrs (left) and 10,000 yrs (right) return periods
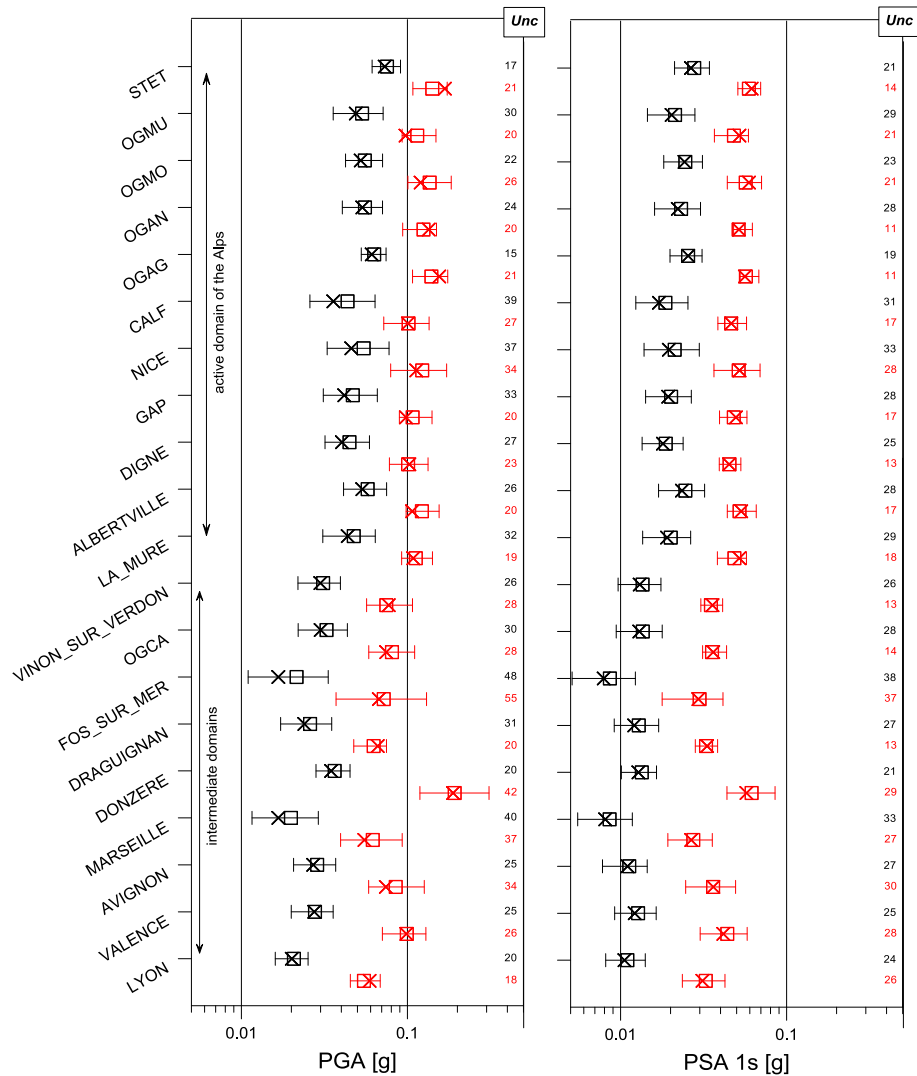
Fig. 19 Comparison of PGAs (left) and spectral accelerations (PSA) at T = 1 s (right) obtained in this study (in black) and in the ESHM13 (in red: bars, 16th–84th fractiles; crosses, medians; and squares, means). Results are for the 20 selected sites for return periods of 475 years and generic rock conditions (Vs30 = 800 m/s). The uncertainty metric Unc = 100*log(PSA$_{84}$/PSA$_{16}$) is shown by numbers in the left vertical axis

minimum magnitude of approximately Mw = 4.5 and consequently, in region of low-to-moderate seismicity, the available seismicity sample is limited, requiring subjective judgment to establish the activity rates parameters. We note that the seismic hazard at Donzere from ESHM13 is surprisingly large compared to the other sites. This site is located close to the Tricastin area characterized by a peculiar seismicity composed by frequent very shallow events of magnitudes around Mw = 3. The ESHM13 provides very large activity rates for this zone that are likely due to overestimated Mw of the historical

earthquakes in the SHEEC catalogue because the adopted procedure did not consider the shallow depth of these events.

The uncertainty metric is globally consistent in both studies and we observe, consistently, large uncertainties at some sites (e.g., Marseille and Fos-sur-Mer).

6 Discussion and conclusions

We outlined the final PSHA conducted within the SIGMA project for the French region of interest (i.e. Southeastern France). The logic tree developed in this study is the results of an extensive set of scientific products provided by the various WPs, of reviews and comments of the deliverables presented to the scientific committee and of discussions with the SIGMA scientific community. The development of this PSHA model was also based on personal experience of the authors in recent PSHA projects in France subjected to review process. The PSHA model presented herein aimed at integrating relevant scientific progress made in the context of SHA for southeastern France since the beginning of the SIGMA project.

The model developed in this study complies with the state-of-the-art of regional PSHA in Europe and worldwide, it will represent a reference for the PSHA practice in France and will set new standards for future studies. The process followed within the SIGMA project finally led to essential changes in both the SSC and GMC logic trees with respect to the pilot model developed at the beginning of the project. The major improvements in the hazard model during the course of the project were:

- The use of the SIGMA earthquake catalogue (FCAT-17, Manchuel et al. 2017) including instrumental and historical seismicity. This provided an instrumental catalogue in Mw and refined estimates of Mw and depth for historical earthquake that are a major source of uncertainties in the development of the hazard model. Moreover, the uncertainties estimates for Mw provided in the catalogue were directly propagated in the calculation of MFDs;
- The assessment of the maximum earthquake magnitude in the study region was defined by applying a Bayesian approach adapted to the French context. This provided a more objective definition of Mmax and its uncertainties and avoided the excessive use of expert judgement.
- The SSC logic tree was improved by considering recent progress in the PSHA practice and recent scientific publications. A fault model for the Middle Durance Fault and compressive faults of the Provence region and smoothed seismicity models were included in the SSC logic tree. The adopted smoothed seismicity model allowed considering spatial variability in the Mmax distributions and spatial constrains for the smoothing kernels (leaky or strict boundaries) over the study region.
- The set of GMPEs used in the GMC logic tree was selected based on outcomes of WP2, devoted to the development of models for the Pan-European region and for the SIGMA area of interest. Moreover, other recent GMPEs, based on global datasets, were included in the logic tree to account for the epistemic uncertainties in the ground motion scaling in France.
- With the use of recent GMPEs including complex distance metrics, a major point of improvement was the consideration of virtual faults and their aleatory variability for AS and smoothed seismicity models.

In this paper, we presented the hazard results for 20 sites in Southeastern France in terms of UHS at two return periods. The results at the different sites were discussed in terms of hazard variability and mean values. In particular, we pointed out that the epistemic uncertainties in the GMC and in the SSC provided similar contribution to the total hazard uncertainties at the considered return periods. We also observed that the smoothed seismicity model generally provide lower spectral accelerations than the AS models for sites in low-seismicity regions.

We compared the hazard estimates obtained in this study with previous results from national (MEDD 2002 and AFPS06) and international (SHARE) projects. The results of this study provided overall lower accelerations at 475 years return periods with respect the other studies. This is primarily related to the selected GMPEs and to the activity rates issued by the earthquake catalogue. At 10,000 years return period the comparison with the AFPS06 model showed overall consistent results although significant differences were observed for some sites either in terms of mean acceleration or of uncertainties. Although the scale of the two target regions is not comparable and the hazard models are largely independent, the differences with respect the ESHM13 were quite surprising. We note, however, that similar results have been reported in a number of national hazard studies, for example Germany and Switzerland; it is explained largely by the choice of the GMPEs in the SHARE project.

Currently, a new hazard model is under development for the whole France, building on the experience of the SIGMA project and on the model presented in this study. While these models provide new insights to conduct a PSHA at regional scale, other studies conducted in the same region and at sites where site-specific data are available (Ameri et al. 2017b) offer new perspectives in implementing partially non-ergodic PSHA. Such new approach highlighted the importance of collecting new local data to establish more reliable site-specific hazard estimates.

References

Abrahamson NA, Silva WJ (2008) Summary of the Abrahamson & Silva NGA ground motion relations. Earthq Spectra 24:67–97

Akkar S, Bommer JJ (2010) Empirical equations for the prediction of PGA, PGV, and spectral accelerations in Europe, the Mediterranean Region, and the Middle East. Seismol Res Lett 81:195–206

Akkar S, Sandikkaya MA, Bommer JJ (2014) Empirical ground-motion models for point- and extended-source crustal earthquake scenarios in europe and the middle east. Bull Earthq Eng 12(1):359–387

Albarello D, Camassi R, Rebez A (2001) Detection of space and time heterogeneity in the completeness of a seismic catalog by a statistical approach: an application to the Italian area. Bull Seismol Soc Am 91:1694–1703

Ambraseys NN, Simpson KA, Bommer JJ (1996) Prediction of horizontal response spectra in Europe. Earthq Eng Struct Dyn 25:371–400

Ameri G (2014) Empirical ground motion model adapted to the French context. SIGMA Deliverable D2-131

Ameri G, Gomes C, Secanell R, Martin C (2014) Integration of sigma improvement for psha and sensibility studies (intermediate results) - SIGMA Deliverable D4-138

Ameri G, Baumont D, Gomes C, Martin C, Secanell R, Le Dortz K, Le Goff B (2015) On the choice of maximum earthquake magnitude for seismic hazard assessment in metropolitan France—insight from the Bayesian approach, 9ème Colloque National AFPS, 30/11-02/12. Marne-la-Vallée, France

Ameri G, Drouet S, Traversa P, Bindi D, Cotton F (2017a) Toward an empirical ground motion prediction equation for France: accounting for regional differences in the source stress parameter. Bull Earthq Eng. doi:10.1007/s10518-017-0171-1

Ameri G, Hollender F, Perron V, Martin C (2017b) Site-specific partially nonergodic PSHA for a hard-rock critical site in southern France: adjustment of ground motion prediction equations and sensitivity analysis. Bull Earthq Eng. doi:10.1007/s10518-017-0118-6

Baize S, Cushing M, Lemeille F, Jomard H (2011) Révision du zonage sismotectonique de la France pour l'évaluation de l'aléa sismique. In: Proceedings du 8ème colloque national AFPS

Baize S, Cushing EM, Lemeille F, Jomard H (2013) Updated seismotectonic zoning scheme of Metropolitan France, with reference to geologic and seismotectonic data. Bulletin de la Société Géologique de France 184(3):225–259

Baumont D, Manchuel K, Traversa P, Durouchoux C, Nayman E, Ameri G (2017) Empirical intensity attenuation models calibrated in Mw for Metropolitan France. Bulletin of Earthquake Engineering (**submitted for this issue**)

Beauval C, Tasan H, Laurendeau A, Delavaud E, Cotton F, Guéguen P, Kuehn N (2012) On the testing of ground-motion prediction equations against small-magnitude data. Bull Seismol Soc Am 102:1994–2007. doi:10.1785/0120110271

Berge-Thierry C, Griot-Pommera DA, Cotton F, Fukushima Y (2003) New empirical response spectral attenuation laws for moderate European earthquakes. J Earthq Eng 7(2):193–222

Bindi D, Massa M, Luzi L, Ameri G, Pacor F, Puglia R, Augliera P (2014) Pan-European ground-motion prediction equations for the average horizontal component of PGA, PGV, and 5%-Damped PSA at Spectral Periods up to 3.0 s using the RESORCE dataset. Bull Earthq Eng 12(1):391–430

Bindi D, Cotton F, Kotha S-R, Bosse C, Stromeyer D, Gruenthal G (2017) Application-driven ground motion prediction equation for seismic hazard assessments in non-cratonic moderate-seismicity areas. J Seismol. doi:10.1007/s10950-017-9661-5

Bles J-L, Bour M, Dominique P, Godefroy P, Martin C, Terrier M (1998) Zonage sismique de la France métropolitaine pour l'application des règles parasismiques aux installations classées. Document BRGM n°279, p.1-56., 8 fig., 5 tabl

Bommer JJ, Stafford PJ, Alarcón JE, Akkar S (2007) The influence of magnitude range on empirical ground-motion prediction. Bull Seismol Soc Am 97(6):2152–2170

Boore DM, Stewart JP, Seyhan E, Atkinson GM (2014) NGA-West 2 equations for predicting PGA, PGV, and 5%-damped PSA for shallow crustal earthquakes. Earthquake Spectra 30:1057–1085

Budnitz RJ, Apostolakis G, Boore DM, Cluff LS, Coppersmith KJ, Cornell CA, Morris PA (1997). Recommendations for probabilistic seismic hazard analysis: guidance on uncertainty and use of experts, NUREG/CR-6372, two volumes, US Nuclear Regulatory Commission, Washington, DC

Burkhard M, Grünthal G (2009) Seismic source zone characterization for the seismic hazard assessment project PEGASOS by the Expert Group 2 (EG 1b). Swiss J Geosci 102(1):149–188

Campbell KW (2016) Comprehensive comparison among the Campbell–Bozorgnia NGA-West2 GMPE and Three GMPEs from Europe and the Middle East. BSSA 106(5):2081–2103

Campbell KW, Bozorgnia Y (2014) NGA-West2 ground motion model for the average horizontal components of PGA, PGV, and 5%-damped linear acceleration response spectra. Earthq Spectra 30(3):1087–1115

Cara M, Cansi Y, Schlupp A et al (2015) SI-Hex: a new catalogue of instrumental seismicity for metropolitan France. Bull Soc Géol Fr 186:3–19

Carbon D, Drouet S, Gomes C, Leon A, Martin Ch, Secanel R (2012) Initial probabilistic seismic hazard model for FRANCE'S SOUTHEAST 1/4-SIGMA Deliverable D4-41

Cauzzi C, Faccioli E (2008) Broadband (0.05 to 20 s) prediction of displacement response spectra based on worldwide digital records. J Seismol 12:453–475

Cauzzi C, Faccioli E, Vanini M, Bianchini A (2015) Updated predictive equations for broadband (0.01–10 s) horizontal response spectra and peak ground motions, based on a global dataset of digital acceleration records. Bull Earthq Eng 13(6):1587–1612

Chiou BS-J, Youngs RR (2008) An NGA model for the average horizontal component of peak ground motion and response spectra. Earthq Spectra 24(1):173–215

Clement C, Scotti O, Bonilla L, Baize S, Beauval C (2004) Zoning versus faulting models in PSHA for moderate seismicity regions: preliminary results for the Tricastin nuclear site, France. Bollettino di Geofisica Teorica ed Applicata 45(3):187–204

Clement C, Carbon D, Martin C, Guignard P, Bellier O (2009) Probabilistic seismic hazard assessment in Western Provence based on a faults seismotectonic model. In: Proceedings colloque Provence 2009

Cotton F, Scherbaum F, Bommer JJ, Bungum H (2006) Criteria for selecting and adjusting ground-motion models for specific target regions: application to central Europe and rock sites. J Seismol 10:137–156. doi:10.1007/s10950-005-9006-7

Cushing M, Bellier O, Nechtschein S, Sebrier M, Lomax A, Volant PH, Dervin P, Guignard P, Bove L (2007) A multidisciplinary study of a slow-slipping fault for seismic hazard assessment: the example of the Middle Durance Fault (SE France). Geophys J Int. doi:10.1111/j.1365-246X.2007.03683.x

Douglas J, Ulrich T, Bertil D, Rey J (2014a) Comparison of the ranges of uncertainty captured in different seismic-hazard studies. Seismol Res Lett 85(5):977–985

Douglas J, Akkar S, Ameri G, Bard P-Y, Bindi D, Bommer JJ, Bora SS, Cotton F, Derras B, Hermkes M, Kuehn NM, Luzi L, Massa M, Pacor F, Riggelsen C, Sandikkaya MA, Scherbaum F, Stafford PJ, Traversa P (2014b) Comparisons among the five ground motion models developed using RESORCE for the prediction of response spectral accelerations due to earthquakes in Europe and the Middle East. Bull Earthq Eng 12:341–358

Drouet S, Cotton F (2015) Regional stochastic GMPEs in low-seismicity areas: scaling and aleatory variability analysis—application to the French Alps. Bull Seismol Soc Am 105(4):1883–1902

Faccioli E, Paolucci R, Vanini M (2015) Evaluation of probabilistic site-specific seismic-hazard methods and associated uncertainties, with applications in the po plain, Northern Italy. Bull Seismol Soc Am 105:2787–2807

Gardner JK, Knopoff L (1974) Is the sequence of earthquakes in Southern California, with aftershocks removed, Poissonian ? Bull Seis Soc Am 64(5):1363–1367

Grünthal G, Arvidsson R, Bosse C (2010) Earthquake model for the European-Mediterranean region for the purpose of GEM1. Scientific Technical report 10/04, GFZ German Research Centre or Geosciences, Potsdam, p 38

Gutenberg B, Richter CF (1956) Magnitude and energy of earthquakes. Ann Geofis 9:1–15

Guyonnet-Benaize C (2011) Modélisation 3d multi-échelles des structures géologiques de la région de la faille de la Moyenne Durance (SE, france). Thèse Université de Provence, Laboratoire de Géologie des Systèmes et Réservoirs Carbonatés

Guyonnet-Benaize C, Lamarche J, Hollender F, Viseur S, Münch P, Borgomano J (2015) Three-dimensional structural modeling of an active fault zone based on complex outcrop and subsurface data: the Middle Durance Fault Zone inherited from polyphaser Meso-Cenozoic tectonics (southeastern France). Tectonics. doi:10.1002/014TC003749

Helmstetter A, Kagan YY, Jackson DD (2007) High-resolution time-independent grid-based forecast for M #5 earthquakes in California. Seismol Res Lett 78:78–86. doi:10.1785/gssrl.78.1.78

Johnston AC, Coppersmith KJ, Kanter LR, Cornell CA (1994) The earthquakes of stable continental regions—assessment of large earthquake potential. Electr Power Res Inst (EPRI), TR-102261-V1, 2–1-98

Le Pichon X, Rangin C (2010) Geodynamic of the France Southeast Basin: importance of gravity tectonics. Thematic issue edited by Le Pichon and Rangin. Bull Soc Géol Fr 181(6):476

Leonard M (2010) Earthquake fault scaling: self-consistent relating of rupture length, width, average displacement, and moment release. Bull Seismol Soc Am 100(5A):1971–1988

Manchuel K, Traversa P, Baumont D, Cara M, Nayman E, Durouchoux C (2017) French historical and instrumental periods earthquake catalogue. Bull of Earthquake Eng. (in press)

Martin C, Secanell R (2006) Développement d'un modèle probabiliste d'aléa sismique calé sur le retour d'expérience, Phase 2: Calculs et cartographie suivant l'arbre logique défini par le groupe « zonage », Document GZ7 produit dans le cadre du groupe de travail AFPS « ZONAGE », Geoter Report, GTR/CEA/0306-294, p 89 (**in French**)

Martin C, Combes P, Secanell R, Lignon G, Carbon D, Fioravanti A, Grellet B (2002) Révision du zonage sismique de la France, Etude probabiliste. GTR/MATE/0701-150, MATE, Paris (in French)

Musson RMW (1999) Probabilistic seismic hazard maps for the North Balkan Region. Ann Geophys 42:1109–1124

Papazachos BC, Scordilis EM, Panagiotopoulos DG, Papazachos CB, Karakaisis GF (2004) Global relations between seismic fault parameters and moment magnitude of earthquakes. In: Proceeding of the 10th international congress, Thessaloniki, April, Bulletin of the Geological Society of Greece Vol. XXXVI, pp 1482–1489

Pecker A, Faccioli E, Gurpinar A, Martin C, Renault P (2017) An overview of the SIGMA research project. Springer, Berlin. doi:10.1007/978-3-319-58154-5

Rangin CL, Le Pichon X, Hamon Y, Loget N, Crepy A (2010) Gravity tectonics in the SE Basin (Provence, France) imaged from seismic reflection data. Bull Soc Géol Fr 181(6):503–530

RFS 2001-01 (2001) French safety rule, published by the French Nuclear Safety Authority, http://www.asn.fr/index.php/Divers/Autres-RFS/RFS-2001-01

Schorlemmer D, Wiemer S, Wyss M (2005) Variations in earthquake-size distribution across different stress regimes. Nature 437:539–542

Stepp JC (1972) Analysis of completeness of the earthquake sample in the Puget Sound area and its effect on statistical estimates of earthquake hazar. Proc Inern Conf Microzonation 2:897910

Terrier M (2006) Identification et hiérarchisation des failles actives de la Région Provence-Alpes-Côte d'Azur, Phase 3: hiérarchisation des failles actives. BRGM, Rapport final, BRGM/RP-53930-FR, p 216

Thomas P, Wong I, Abrahamson N (2010) Verification of probabilistic seismic hazard analysis computer programs. In: PEER Rept. 2010/106, pacific earthquake Engineering Research Center, University of California, Berkeley, California, USA

Thouvenot F, Frechet J, Jenatton L, Gamond JF (2003) The belledonne border fault: identification of an active seismic strike-slip fault in the western Alps. Geophys J Int 155:174–192

Thouvenot F, Jenatton L, Gratier JP (2009) 200-m-deep earthquake swarm in Tricastin (lower Rhône Valley, France) accounts for noisy seismicity over past centuries. Terra Nova 21:203–210

Traversa P, Baumont D, Manchuel K, Nayman E Durouchoux C (2017) Magnitude and depth estimation for historical earthquakes, methodology and application to the French seismicity. Bull Earthq Eng, this issue

Van Stiphout T, Zhuang J, Marsan D (2012) Seismicity declustering, community online resource for statistical seismicity analysis. doi: 10.5078/corssa-52382934. Available at http://www.corssa.org

Vanini M, Corigliano M, Faccioli E, Figini R, Luzi L, Pacor F, Paolucci R (2017) Improving seismic hazard approaches for critical infrastructures: a pilot study in the po plain. Bull Earthq Eng. doi:10.1007/s10518-017-0102-1

Weichert DH (1980) Estimation of the earthquake recurrence parameters for unequal observation periods for different magnitudes. Bull Seismol Soc Am 70(4):1337–1346

Wells DL, Coppersmith KJ (1994) New empirical relationships among magnitude, rupture length, rupture width, rupture area, and surface displacement. Bull Seismol Soc Am 84:974–1002

Wesnousky SG (2008) Displacement and geometrical characteristics of earthquake surface ruptures: issues and implications for seismic-hazard analysis and the process of earthquake rupture. Bull Seismol Soc Am 98(4):1609–1632

Wheeler RL (2009) Methods of Mmax estimation east of the rocky mountains, U.S. Geological Survey Open-File Report 2009–1018, p 44

Woessner et al (2015) The 2013 European seismic hazard model: key components and results. Bull Earthq Eng 13(12):3553–3596

Youngs RR, Coppersmith K (1985) Implications of fault slip rates and earthquake recurrence models to probabilistic seismic hazard estimates. Bull Seism Soc Am 58:939–964

Zhao JX, Zhang J, Asano A, Ohno Y, Oouchi T, Takahashi T, Ogawa H, Irikura K, Thio HK, Somerville PG, Fukushima Yasuhiro, Fukushima Yoshimitsu (2006) Attenuation relations of strong ground motion in Japan using site classification based on predominant period. Bull Seismol Soc Am 96:898–913